Available online at www.sciencedirect.com
ScienceDirect
Icarus 184 (2006) 39–58
ICARUS
www.elsevier.com/locate/icarus

Terrestrial planet formation with strong dynamical friction

David P. O'Brien [a,b,*], Alessandro Morbidelli [a], Harold F. Levison [c]

[a] *Observatoire de Nice, B.P. 4229, 06304 Nice Cedex 4, France*
[b] *Planetary Science Institute, 1700 E. Ft. Lowell, Suite 106, Tucson, AZ 85719, USA*
[c] *Department of Space Studies, Southwest Research Institute, 1050 Walnut St., Suite 400, Boulder, CO 80302, USA*

Received 30 November 2005; revised 6 April 2006

Available online 9 June 2006

Abstract

We have performed 8 numerical simulations of the final stages of accretion of the terrestrial planets, each starting with over 5× more gravitationally interacting bodies than in any previous simulations. We use a bimodal initial population spanning the region from 0.3 to 4 AU with 25 roughly Mars-mass embryos and an equal mass of material in a population of ∼1000 smaller planetesimals, consistent with models of the oligarchic growth of protoplanetary embryos. Given the large number of small planetesimals in our simulations, we are able to more accurately treat the effects of dynamical friction during the accretion process. We find that dynamical friction can significantly lower the timescales for accretion of the terrestrial planets and leads to systems of terrestrial planets that are much less dynamically excited than in previous simulations with fewer initial bodies. In addition, we study the effects of the orbits of Jupiter and Saturn on the final planetary systems by running 4 of our simulations with the present, eccentric orbits of Jupiter and Saturn (the EJS simulations) and the other 4 using a nearly circular and co-planar Jupiter and Saturn as predicted in the Nice Model of the evolution of the outer Solar System [Gomes, R., Levison, H.F., Tsiganis, K., Morbidelli, A., 2005. Nature 435, 466–469; Tsiganis, K., Gomes, R., Morbidelli, A., Levison, H.F., 2005. Nature 435, 459–461; Morbidelli, A., Levison, H.F., Tsiganis, K., Gomes, R., 2005. Nature 435, 462–465] (the CJS simulations). Our EJS simulations provide a better match to our Solar System in terms of the number and average mass of the final planets and the mass-weighted mean semi-major axis of the final planetary systems, although increased dynamical friction can potentially improve the fit of the CJS simulations as well. However, we find that in our EJS simulations, essentially no water-bearing material from the outer asteroid belt ends up in the final terrestrial planets, while a large amount is delivered in the CJS simulations. In addition, the terrestrial planets in the EJS simulations receive a late veneer of material after the last giant impact event that is likely too massive to reconcile with the siderophile abundances in the Earth's mantle, while the late veneer in the CJS simulations is much more consistent with geochemical evidence.

Keywords: Accretion; Planetary formation; Terrestrial planets

1. Introduction

The accretion of the terrestrial planets in our Solar System has been the subject of much study, yet is far from being completely understood (see Chambers, 2004, for a recent and thorough review of the field). The basic model for terrestrial planet formation, generally termed the *planetesimal theory*, holds that the formation proceeded through three main stages (which of course overlap with one-another to some degree).

First, dust in the early solar nebula settles to the mid-plane of the nebula and accretes together to form small solid bodies called *planetesimals*. This is currently the least-understood phase of planet formation, with several competing theories. The first is that planetesimals form as the result of gravitational instability in the solar nebula, in which solids are sufficiently concentrated that planetesimals are able to form purely by self-gravity (e.g., Goldreich and Ward, 1973; Ward, 2000; Youdin and Shu, 2002). The second is that planetesimals form by the direct collisional accretion between colliding particles (e.g., Weidenschilling, 1980; Weidenschilling and Cuzzi, 1993; Wurm et al., 2001). While this phase of planet formation still remains to be fully quantified, the key point is that once these

* Corresponding author. Fax: +1 520 795 3697.
E-mail address: obrien@psi.edu (D.P. O'Brien).

0019-1035/$ – see front matter
doi:10.1016/j.icarus.2006.04.005

planetesimals reach a size where they can gravitationally perturb each other, generally on the order of a few km, their orbits begin to cross.

In the second stage, which is much better understood, collisions between planetesimals on crossing orbits lead to the growth of larger *planetary embryos*. The growth of planetary embryos initially proceeds by a process called *runaway accretion* (e.g., Greenberg et al., 1978; Wetherill and Stewart, 1989; Kokubo and Ida, 1996; Weidenschilling et al., 1997). In a swarm of planetesimals, the relative velocity $v_{\rm rel}$ is governed by their frequent encounters with one another, and given their small gravity, is kept low. When one body starts to grow larger than the others, its geometric cross section as well as its gravitational field strengthens, allowing it to sweep up more and more planetesimals.

Runaway growth is stalled somewhat when the planetary embryos grow large enough that their gravitational perturbations on the planetesimals become the dominant influence on $v_{\rm rel}$. The system enters a regime called *oligarchic growth* (e.g., Kokubo and Ida, 1998) in which neighboring embryos are forced to grow at similar rates. When a body starts to grow larger than its neighbors, it begins to increase the $v_{\rm rel}$ of planetesimals in its vicinity, decreasing its accretion efficiency, and thus letting its neighbors catch up. The end result of this stage is a system of roughly comparably sized and spaced planetary embryos embedded in a swarm of planetesimals with a total mass roughly comparable to the total mass of embryos.

In the third and final stage of terrestrial planet accretion, the gravitational effect of the planetesimals begins to fade as their numbers decrease, and the planetary embryos begin to perturb one another onto crossing orbits. Planets then begin grow from collisions between embryos and the accretion of remaining planetesimals. This stage is characterized by relatively violent, stochastic large collisions as compared to the previous stages, where the continual accretion of small bodies dominates. At the same time, while the number of embryos involved (on the order of 50) is easily modeled by direct numerical simulation, the total number of bodies involved, when one includes a realistic number of remnant planetesimals, is still pushing the limits of modern computer workstations.

Numerical modeling of the final stage of terrestrial planet accretion has succeeded in producing systems of terrestrial planets, but these systems are inevitably different from the terrestrial planets in our Solar System. Direct N-body simulations (e.g., Chambers and Wetherill, 1998; Agnor et al., 1999; Chambers, 2001; Raymond et al., 2004) incorporating ∼50–200 bodies generally form about the right number of planets (although generally not a small 'Mercury' and 'Mars'), but those planets are significantly more dynamically excited (i.e., larger eccentricity e and inclination i) than the terrestrial planets in our Solar System and, on average, take too long to form compared to geochemical estimates of the Earth's accretion timescale (Halliday et al., 2000; Kleine et al., 2002; Yin et al., 2002). It has been suggested that the low-density remnant of the decaying solar nebula could provide a damping mechanism via tidal torques on the growing terrestrial planets (Agnor and Ward, 2002). Models of such a scenario, however, while yielding final terrestrial planets with lower eccentricities on a somewhat more reasonable timescale, generally form 6 or 7 planets (Kominami and Ida, 2002, 2004).

It has been noted by Chambers and Wetherill (1998) and Chambers (2001) that including a population of less-massive planetesimals in addition to the massive embryos in direct N-body integrations can potentially decrease the formation timescales and dynamical excitations of the final terrestrial planets. The presence of such a population of remnant planetesimals is predicted by numerical simulations of oligarchic growth of planetary embryos (e.g., Kokubo and Ida, 1998). The key physical process involved is generally termed *dynamical friction* (e.g., Wetherill and Stewart, 1993). As a result of equipartition of energy between gravitationally interacting bodies, the smaller ones get higher relative velocities and the larger ones get lower relative velocities. The relative velocities of embryos will therefore be kept low by dynamical friction, increasing their mutual gravitational focusing and hence increasing their likelihood of colliding and accreting.

Levison et al. (2005) demonstrated that the damping of the embryos provided by dynamical friction can lead to the formation of planets with a dynamical excitation comparable to that of the terrestrial planets in our Solar System. These authors used an N-body integrator that was modified to use individual tracer particles to represent and follow swarms of planetesimals, such that the collective effects of very large numbers of small particles on the accretion process can be treated. In addition, their model allowed for the regeneration of small bodies in large impacts, which has been shown to be a likely outcome of giant impacts (e.g., Agnor and Asphaug, 2004), and keeps the effect of dynamical friction from diminishing as the original population of planetesimals is accreted.

Accurately modeling dynamical friction in the context of a pure N-body simulation, however, requires computers fast enough to numerically integrate a system of a thousand or more bodies in a reasonable amount of time (a larger number of bodies with smaller individual masses will be more realistic). Only recently has this level of computing power become widely available and affordable. Thus, a primary motivation of this work is to explore the effects that using a larger number of smaller planetesimals, and hence an improved treatment of dynamical friction, will have on direct numerical integrations of terrestrial planet formation.

The Chambers (2001) simulations incorporate some of the largest number of interacting bodies to date, and hence produce some of the most reasonable systems of terrestrial planets. Thus, we build on the initial conditions of their simulations with a bimodal population consisting of embryos and planetesimals and increase the number of planetesimals by a factor of 4, keeping a 1:1 ratio between the amount of mass in the embryo and planetesimal sub-populations as used by Chambers. However, Chambers only treats the region from ∼0.5 to 2 AU. To more accurately model the terrestrial planet accretion process, especially in terms of the delivery of water and other volatile material from the region beyond 2.5 AU (referred to here as the 'outer asteroid belt'), we extend the initial distribution of embryos and planetesimals out to 4 AU. Our simulations thus incorporate 25

embryos with roughly the mass of Mars and ∼1000 planetesimals 1/40 as massive, such that the populations of embryos and planetesimals each have the same total mass.

In the limiting case where there are planetary embryos embedded in a very large number of very small planetesimals, the damping of relative velocities by dynamical friction should be independent of the mass of the individual planetesimals and only depend on the surface mass density of the planetesimal swarm. However, before that limit is reached, decreasing the individual planetesimal mass while proportionately increasing their number (hence keeping the same surface mass density) will cause the effects of dynamical friction to become more pronounced. The simulations we perform here are still in that regime, and hence we refer frequently in this paper to "increased" or "stronger" dynamical friction, and "increased damping" that results from using a larger number of bodies in our simulations. In this paper we focus primarily on the effects of this increased dynamical friction—a more detailed description of the mechanism of dynamical friction will appear in Levison et al. (2006, in preparation).

In addition to simply studying the effects of increased dynamical friction, we were also motivated to explore in detail the effects of the orbits of Jupiter and Saturn on the final terrestrial planets. Recent work by Gomes et al. (2005), Tsiganis et al. (2005), and Morbidelli et al. (2005) strongly suggests that the initial system of outer planets was very compact (all within 15 AU of the Sun). After a slow orbital evolution due to interactions with the trans-neptunian disk of planetesimals for hundreds of Myr, Jupiter and Saturn cross their mutual 2:1 mean-motion resonance, triggering the late heavy bombardment (LHB), capturing the current Trojan asteroid populations, and rapidly evolving to their current orbital configuration. While the model does not explicitly require that Jupiter and Saturn have essentially zero e and i at the beginning, they could not be close to their current eccentricities or the system would immediately become unstable. That model will be referred to here as the Nice Model, since all of the authors of that work were at the Observatoire de Nice during the time it was developed.

Other researchers have studied the effects that different orbits of the outer planets can have on terrestrial planet formation. Chambers and Cassen (2002) and Raymond et al. (2004) found that increasing Jupiter and Saturn's eccentricity by a factor of 2 leads to a smaller contribution of material from beyond 2.5 AU to the terrestrial planets, due to much more rapid clearing of the asteroid belt. However, they also found that the masses and locations of the terrestrial planets are best reproduced when Jupiter and Saturn had a larger e than their current values. Levison and Agnor (2003) studied a wide range of possible giant planet systems and demonstrated that different giant planet configurations can lead to substantially different terrestrial planet systems, although the issue of composition was not treated in detail.

Thus, the configuration of Jupiter and Saturn during terrestrial planet formation could have left a signature on the final terrestrial planet system. In the Chambers and Cassen (2002), Levison and Agnor (2003) and Raymond et al. (2004) work, the simulations were limited to ∼100–200 bodies by the computers of the time, such that the effects of dynamical friction are not accurately treated. Here we study in detail, with ∼1000-body simulations that can accurately account for dynamical friction, the effects on the final system of terrestrial planets in the case where Jupiter and Saturn begin on their present orbits and in the case where they begin on the nearly circular, co-planar orbits predicted before the onset of the LHB in the Nice Model.

In Section 2 we describe the code and the initial conditions used for our simulations. The results of our simulations are described in detail in Section 3. In Section 4, we interpret and explain the trends seen in our simulations, specifically with regards to the effects of increased dynamical friction and the effects of the orbits of Jupiter and Saturn. Finally, in Section 5, we summarize our results and highlight their implications for the Nice Model, the origin of the Earth's volatiles, the formation of the Moon, and terrestrial planet accretion in general.

As we were preparing this paper for submission, we learned at the editorial level that a pair of papers that are also on the subject of high-resolution simulations of terrestrial planet formation had been submitted by another group (Raymond et al., 2005a, 2005b). Of their simulations, their 'Simulation 2' initial conditions are the most similar to those used here in that their embryos and planetesimals both extend throughout the entire terrestrial planet and asteroid belt region, although they use a mass ratio of 2:1 between the populations of embryos and planetesimals, while we use a 1:1 ratio, and they only consider the case of a circular Jupiter. Having more mass in the planetesimal population (i.e., a larger surface mass density of planetesimals) gives more dynamical friction, and we believe this is the reason that our simulations produce somewhat less eccentric planets than their Simulation 2.

Raymond et al. (2005a, 2005b) suggest that having embryos in the asteroid belt, as in our simulations and their Simulation 2, is unlikely, since their 'Simulation 0,' which starts with ∼1900 interacting bodies of ∼0.005 M_e each, fails to form a significant number of large embryos outwards of 2.5 AU before Jupiter's likely formation time (a few Myr). However, they note that this is a model-dependent result. In particular, their simulation started with a fully-accreted Jupiter, which would immediately stir up the asteroid belt region and inhibit the growth of embryos there. The fact that Jupiter's ∼10 Earth-mass core was able to accrete in our Solar System beyond the asteroid belt suggests that embryos were likely able to accrete in the asteroid belt, even accounting for the roughly 3–4× decrease in the mass density of solid material inside the snow line (Thommes et al., 2003). In addition, taking into account much smaller bodies than treated in the Raymond et al. (2005a, 2005b) Simulation 0 can drastically lower the formation time for planetary embryos. Numerical simulations using a multi-zone accretion code that accounts for bodies down to ∼15 km in diameter are able to form Mars-mass embryos around 1 AU in ∼1 Myr (Weidenschilling et al., 1997), and more recent simulations accounting for bodies down to ∼1 km in diameter are able to form Mars-mass embryos out to 4 AU on a timescale of ∼1 Myr (S.J. Weidenschilling, pers. comm.). Thus, there is good reason to believe that Mars-mass planetary embryos existed through-

out the entire inner Solar System, as assumed in our initial conditions.

2. Method

For our simulations, we use SyMBA (Duncan et al., 1998), which is a symplectic N-body integrator that handles close encounters. SyMBA allows for a population of gravitationally interacting massive bodies as well as a population of less-massive bodies that interact with the massive bodies but not with one another. In addition, when two bodies collide, they are merged together, conserving linear momentum. Hence, it is an ideal tool for modeling the final stage of terrestrial planet accretion, in which there is a population of massive embryos and a much more numerous population of less-massive planetesimals.

For our initial distribution of planetary embryos and planetesimals in our simulations, we use a distribution based on that of Chambers (2001) (their Simulations 21–24). That work was chosen as a starting point because their simulations, to date, have resulted in some of the most reasonable systems of terrestrial planets as compared to our own Solar System.

The surface density profile of the distribution is $\Sigma(r) = \Sigma_0(r/1\ \mathrm{AU})^{-3/2}$, with $\Sigma_0 = 8\ \mathrm{g\,cm^{-2}}$, and drops linearly to zero between 0.7 and 0.3 AU. Bodies are distributed in semi-major axis strictly according to this density profile, with half of the mass in large bodies of 0.0933 M_e, which is roughly the mass of Mars, and the other half of the mass in bodies 1/40 as massive (Chambers (2001) used a factor of 1/10). Initial eccentricities and inclinations are randomly chosen from a uniform distribution between 0°–0.01° and 0°–0.5°, respectively, and the other angular orbital elements randomly distributed between 0° and 360°. This distribution is extended out to 4 AU (the Chambers (2001) simulations were truncated at 2 AU). The total Mass in the disk is ∼4.7 M_e, with ∼2.6 M_e inside of 2 AU. Fourteen embryos and ∼550 planetesimals lie inside of 2 AU.

We performed 2 sets of 4 simulations with this initial distribution, using different random number seeds to generate the exact orbital parameters in each of the simulations. A timestep of 7 days was used, and the simulations were run for 250 Myr each. Each simulation required roughly 1 month of computing time on an Opteron workstation. The major limitation of the SyMBA algorithm is that it is not able to treat close encounters with the Sun. Hence, bodies with a perihelion less than 0.1 AU were assumed to hit the Sun and were discarded. Furthermore, those with an aphelion greater than 10 AU (i.e., crossing both Jupiter and Saturn) were assumed to be ejected from the system.

In the first set of simulations, denoted here as CJS1-4 (for 'Circular Jupiter and Saturn'), we adopt the initial orbits of Jupiter and Saturn that were found to best reproduce the timing of the late heavy bombardment in the Nice Model: $a_j = 5.45$, $a_s = 8.18$, $e_j = e_s = 0$, $i_j = 0$, and $i_s = 0.5°$. In this case, Jupiter is somewhat further out than its current position and Saturn is closer to the Sun. As noted previously, somewhat larger e and i are not necessarily inconsistent with the Nice Model, although e_j and e_s comparable to their current values would make the system immediately unstable. The embryos and planetesimals are centered on the plane of Jupiter's initial orbit. Using the Jupiter plane rather than the invariant plane in this case makes little difference. Since those two planes are only inclined a few tenths of a degree to one another and the mass of embryos and planetesimals is tiny compared to Jupiter and Saturn, the simulation rapidly becomes indistinguishable from one where they start on the invariant plane. Migration of Jupiter and Saturn is not included in these simulations, because terrestrial planet accretion would be over well before the LHB occurs (triggered by Jupiter and Saturn crossing their mutual 2:1 mean-motion resonance), and migration before the LHB is slow compared to the migration of the planets in the time immediately following the 2:1 resonance crossing. In the second set of simulations, denoted here as EJS1-4 (for 'Eccentric Jupiter and Saturn'), we use the current orbits of Jupiter and Saturn, and the embryos and planetesimals are centered on the invariant plane of Jupiter and Saturn. In both sets of simulations, Jupiter and Saturn are included from the beginning, as in the Chambers (2001) simulations.

We used a timestep that is common in the literature for this type of simulation using SyMBA or similar integrators such as Mercury (Chambers, 1999). For example, Chambers and Wetherill (1998) use 10 days, Chambers (2001) uses 7 days, and Raymond et al. (2004, 2005a, 2005b) use 6 days. However, we realized in retrospect that such a timestep was likely too large. In general, SyMBA and similar integrators require a timestep that is less than ∼1/20 of the orbital period at the perihelion distance if the perihelion passage is to be resolved accurately (Levison and Duncan, 2000). For a 7 day timestep, bodies with a perihelion distance smaller than 0.5 AU may therefore not be resolved correctly in our simulations, or in other published simulations using similar integrators with comparable timesteps.

Since embryos in our simulations, for the most part, remain relatively dynamically cold, few are likely to suffer close perihelion passages. Those that do are primarily those that enter the 3:1 or ν_6 resonance and are driven into the Sun, which happens quickly enough that numerical errors have little effect. However, some planetesimals, even if not in a resonance, may be kicked onto low-perihelion orbits by encounters with the embryos and remain on those orbits long enough that errors may build up. The effect of this is that those bodies have their semi-major axes raised to Jupiter-crossing values and are ejected from the system. Hence, the primary effect of a too-large timestep is that some fraction of planetesimals were likely artificially ejected from our systems, effectively giving the same result as setting the perihelion cutoff to a larger value. However, even though this may happen on occasion, we believe that the overall effect of this process will be small.

3. Results

In each of our simulations, a stable system of terrestrial planets is formed within 250 Myr and no unstable embryos remain. In 7 out of 8 cases, no planets are formed substantially outside of 2 AU (although a few form just outside of 2 AU, such that the asteroid belt region would be compressed relative to that in our

Solar System). However, in simulation EJS2, a single-embryo planet forms at 3.2 AU, possibly enters into the 2:1 resonance with Jupiter for several tens of Myr, and remains stable at 3.19 from 50 Myr to the end of the simulation at 250 Myr. It is interesting to note that we only have one case out of all 8 simulations where an embryo remains in the asteroid belt region. Previous simulations, incorporating far fewer bodies than ours, frequently have an embryo remaining in the belt. For example, Chambers and Wetherill (1998, 2001) find that an embryo remains in the asteroid belt region in about 1/3 of their simulations.

The dynamical evolution of the asteroid belt region is explored in detail in a separate paper of O'Brien et al. (2006, in preparation). Here, we focus on the evolution of the terrestrial planet region and the characteristics of the final terrestrial planets, which for our purposes include all planets except the single-embryo planet remaining at 3.19 AU in simulation EJS2. The results of our simulations are described in the following subsections. As our results can be interpreted in terms of several underlying themes, we reserve the majority of our interpretations for Section 4, in which we present a unified interpretation of all of our results. Similarly, the implications of our results are discussed in detail in Section 5.

3.1. Fates of planetesimals and embryos

Tables 1 and 2 summarize what happens to the planetesimals and embryos in each of our sets of simulations. There are several obvious differences between the two sets of simulations. First, more bodies, both planetesimals and embryos, are lost from the system in the EJS simulations than in the CJS simulations. In the CJS set of simulations, 60% of the initial mass of embryos and planetesimals ends up in the final system of planets, while in EJS set of simulations, only 44% of the mass ends up in the planets. Second, many more of the bodies that are lost from the system in the EJS set of simulations are lost by colliding with the Sun. In both sets of simulations ∼2% of the planetesimals remain at the end of the simulations. Some of these are on unstable orbits and will likely be ejected or accreted eventually. Others lie on stable orbits in the asteroid belt region.

Table 1
Fates of planetesimals in our two sets of simulations

	CJS	EJS
Ejected from system	46%	33%
Hit Sun	5%	28%
Accreted into planets	45%	35%
Accreted then lost	2%	2%
Still floating around	2%	2%

Table 2
Fates of embryos in the two sets of simulations

	CJS	EJS
Ejected from system	20%	31%
Hit Sun	0%	11%
Accreted into planets	76%	55%
Accreted then lost	4%	3%

Note that the embryo that remains stable in the asteroid belt in simulation EJS2 is counted under 'Accreted into planets.'

3.2. Number, mass, and orbits of the planets

Fig. 1 shows the orbital elements of the terrestrial planets formed in each of our simulations, averaged over the last 10 Myr of each simulation. The masses of the final planets are shown in Fig. 2.

For the CJS set of simulations, the median (and mean) number of planets formed is 3, with a median mass of 0.80 M_e (ranging from 0.36 to 1.57 M_e). For the EJS set of simulations, the median (and mean) number is 3.5 with a median mass of 0.63 M_e (ranging from 0.11 to 0.99 M_e). The median mass of the 4 terrestrial planets in our Solar System is 0.46 M_e (their individual masses are 0.06, 0.81, 1.0, and 0.11 M_e). Thus, an obvious distinction between the two sets of simulations is that those with a circular Jupiter and Saturn tend to produce systems with fewer, more massive planets.

The smallest planet in the CJS set of simulations is ∼3 times more massive than Mars. The EJS set of simulations produces 3 Mars-mass planets (consisting of just one embryo and a few planetesimals). In one case the Mars-mass planet is the innermost planet and in one case it is the outermost. Mercury-mass planets cannot be produced in our simulations because our embryos begin with about the mass of Mars (twice as massive as Mercury).

For the CJS set of simulations, the mass-weighted mean semi-major axis (hereafter referred to as the center of mass) of the final systems of terrestrial planets has a median value of 1.15 AU (ranging from 1.10–1.18 AU), while for the EJS set of simulations, the median value is 0.94 AU (ranging from 0.86–1.01 AU). Thus, simulations with a circular Jupiter and Saturn tend to produce systems of terrestrial planets that have their mass concentrated further away from the Sun. The center of mass of the actual terrestrial planets is at 0.90 AU, although similarities and differences between this and the values for systems in our simulations could be due in part to our choice of the initial surface density profile in addition to the orbits of Jupiter and Saturn.

The spacing of the final planets can be characterized in terms of their separation in mutual Hill radii, $R_{\rm HM}$, where

$$R_{\rm HM} = \left(\frac{m_1 + m_2}{3M_{\rm Sun}}\right)^{1/3}\left(\frac{a_1 + a_2}{2}\right) \quad (1)$$

(Chambers and Wetherill, 1998). For the CJS set of simulations, the final planets have a median orbital spacing of 43 $R_{\rm HM}$ (ranging from 24 to 57 $R_{\rm HM}$). For the EJS set of simulations, the median value is 40 $R_{\rm HM}$ (ranging from 21 to 106 $R_{\rm HM}$). For the actual terrestrial planets, the median value is 40 $R_{\rm HM}$ (26–63 $R_{\rm HM}$). The configuration of Jupiter and Saturn therefore seems to have little influence over this parameter, and both

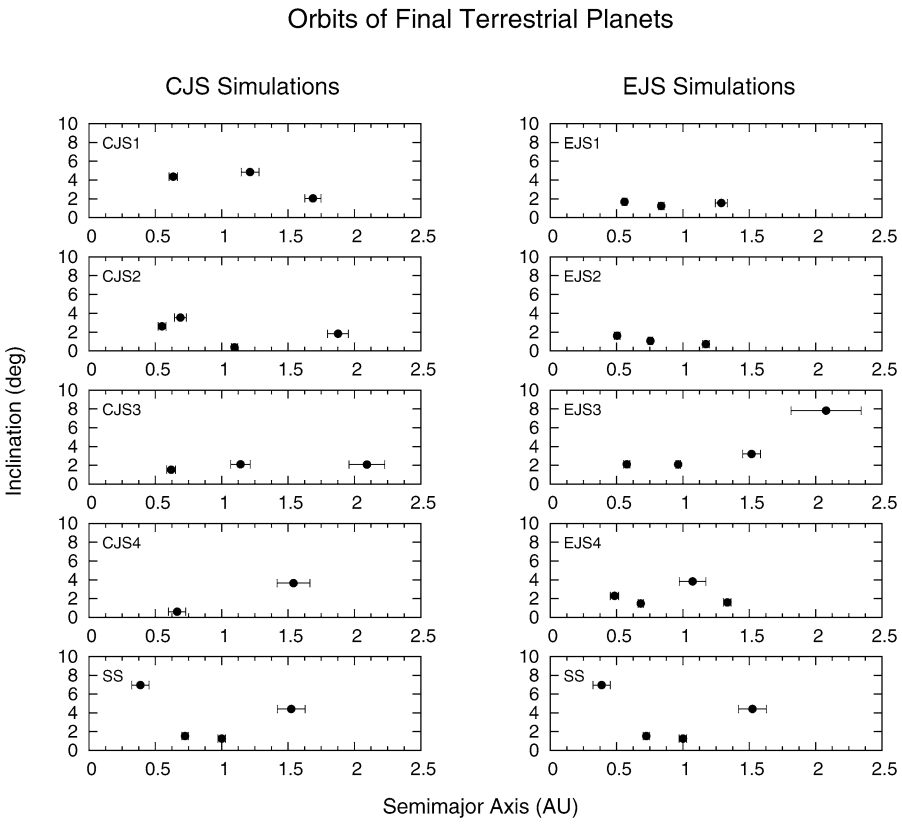

Fig. 1. Orbits of the terrestrial planets formed in each of our simulations. The horizontal bars give the range between perihelion and aphelion. The last panel in each column, labeled 'SS,' is for the terrestrial planets in our Solar System. All orbital elements are in reference to the invariant plane of the Solar System.

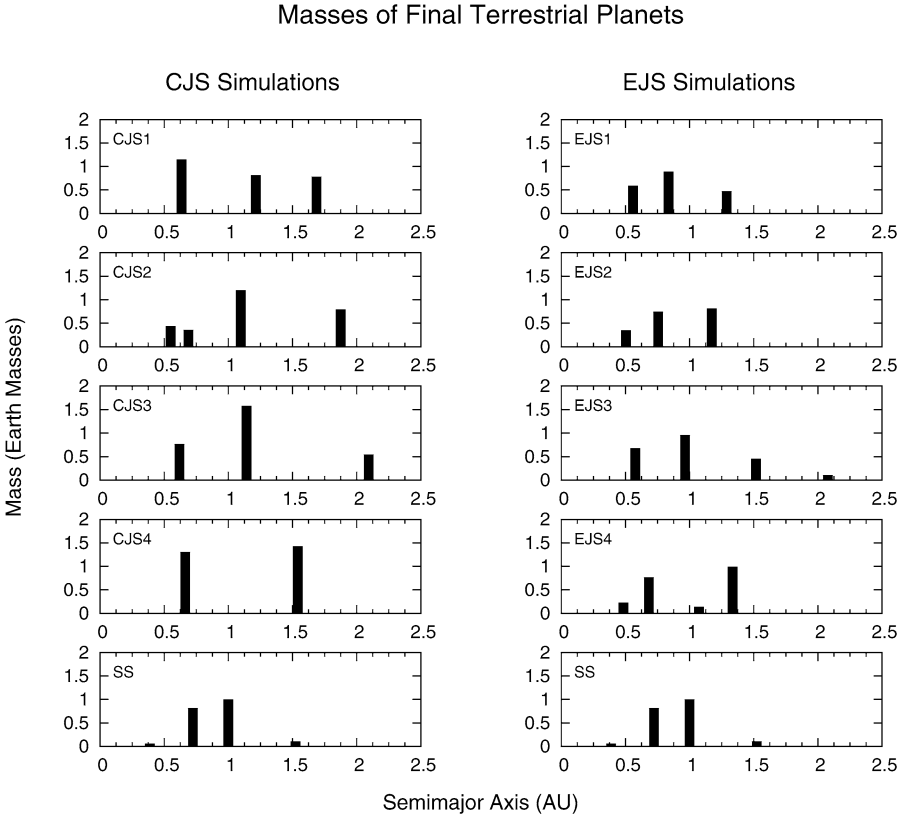

Fig. 2. Masses of the terrestrial planets formed in each of our simulations. The last panel in each column, labeled 'SS,' is for the terrestrial planets in our Solar System.

sets of simulations have a median spacing very close to that of the actual terrestrial planets.

In summary, the planetary systems formed in the CJS simulations have, on average, a smaller number of more-massive planets than in the EJS simulations, and the center of mass of those systems is further from the Sun than in the EJS simulations. However, the fact that the planetary systems formed in the EJS simulations are more compact is offset by the smaller average mass of the individual planets in those simulations, such that the median spacing of the planets in terms of $R_{\rm HM}$ is essentially the same in the CJS and EJS simulations. The interpretation of these results, as well as the interpretation of all of the results presented in this section, are discussed in Section 4.

Two more issues deserve mention here. First, in simulation CJS2, we find that the two inner planets exist close to a 7:5 mean-motion resonance for most of the simulation and actually enter into the resonance at ∼230 Myr, where they stay for the remainder of the simulation. This appears to be triggered when the last stray embryo collides with the third planet at ∼230 Myr, which in turn slightly perturbs the second planet into resonance with the first. When we extend the simulation out to 300 Myr, we find that the planets continue to remain in resonance. To our knowledge, this is the first time a resonant pair of terrestrial planets has been formed in a pure N-body simulation (although resonant giant planets have been formed in other N-body simulations, e.g., Levison et al., 1998), suggesting that such an occurrence is possible, but infrequent.

Finally, it is important to note that the ejection of planetesimals and embryos from the system, primarily by Jupiter, causes the orbits of Jupiter and Saturn to change. In the CJS set of simulations, Jupiter's semi-major axis decreases by ∼0.025 AU over the course of the simulation, while there is negligible change in Saturn's. As their e and i are initially very low, there is negligible change in those values for either planet. Jupiter and Saturn's orbits thus begin and remain essentially circular and co-planar throughout the simulations. In the Nice Model, Jupiter and Saturn slowly migrate due to interactions with a trans-Neptunian disk of planetesimals until they cross their mutual 2:1 mean–motion resonance (long after terrestrial planet accretion is finished), which among other things excites the outer planets to their current orbital configuration and triggers the late heavy bombardment. Thus, having Jupiter and Saturn nearly circular and co-planar during terrestrial planet formation is consistent with their current large e and i in the context of the Nice Model.

In the EJS simulations, Jupiter's semi-major axis also decreases by ∼0.025 AU. In addition, its initial e of ∼0.05 decreases to ∼0.01 and its initial i of and ∼0.35° (relative to the invariant plane) decreases to ∼0.025°. There is negligible change in a for Saturn, but its e drops from ∼0.05 to ∼0.015 and i drops from ∼0.9° (relative to the invariant plane) to ∼0.1°. The timescale for these changes in the EJS simulations is on the order of 50 Myr. Thus, as also noted by other researchers (e.g., Petit et al., 2001; Chambers and Cassen, 2002), if no other mechanisms are invoked to enhance the eccentricity and inclination of Jupiter and Saturn after the formation of the terrestrial planets, they must start out with e and i larger than their present values by about a factor of two in order to end up in their current configuration. Starting Jupiter and Saturn on even more eccentric and inclined orbits than used in the EJS simulations here would likely lead to even more profound differences when compared to our CJS set of simulations.

3.3. Dynamical excitation of final planetary systems

The degree of excitation of a planetary system can be quantified as the relative angular momentum deficit (AMD), denoted S_d:

$$S_d = \frac{\sum_j m_j \sqrt{a_j(1-e_j^2)}\cos i_j - \sum_j m_j \sqrt{a_j}}{\sum_j m_j \sqrt{a_j}} \tag{2}$$

(Laskar, 1997), where m_j, a_j, e_j, and i_j are the mass, semi-major axis, eccentricity, and inclination of planet j. This quantity is the normalized difference between the Z-component of the angular momentum of the system and the angular momentum of the system if all e and i were zero. Table 3 shows the angular momentum deficits of the systems formed in our simulations, using orbital elements averaged over the last 10 Myr of the simulations. The median AMD is −0.0030 in the CJS simulations and −0.0010 in the EJS simulations. The angular momentum deficit of the actual terrestrial planets is −0.0018 when averaged over million-year timescales (Chambers, 2001).

Levison et al. (2005), using an N-body integrator modified to follow swarms of planetesimals using tracer particles, showed that dynamical friction could produce final terrestrial planets with a dynamical excitation comparable to those in our Solar System. Our direct N-body simulations achieve comparable results, yielding systems that are on average much less dynamically excited, and hence much closer to the actual terrestrial planets in our Solar System, than any previous direct N-body simulations.

For comparison, the Chambers and Wetherill (1998) Model C simulations, each consisting of at most ∼50 bodies extending out to 4 AU and assuming the present orbits of Jupiter and Saturn, yield a median AMD of −0.033. The Chambers (2001) Simulations 21–24, each consisting of ∼150 bodies and also assuming the present Jupiter and Saturn, have a median AMD of −0.0050. Those simulations only extended out to 2 AU, and it is likely that their AMD would be even higher

Table 3
Angular momentum deficits S_d of the final terrestrial planet systems formed in each simulation, using orbital elements averaged over the last 10 Myr of each simulation

	S_d (CJS)	S_d (EJS)
1	−0.0034	−0.00077
2	−0.0013	−0.00049
3	−0.0026	−0.0026
4	−0.0051	−0.0013
Median	−0.0030	−0.0010

For comparison, the angular momentum deficit of the actual terrestrial planets is −0.0018 when averaged over million-year timescales.

if they were extended out to 4 AU (e.g., the Chambers and Wetherill (1998) Model C Simulations, which extend out to 4 AU, have a median AMD ∼50% larger than in their Model B simulations, which only extend to 1.8 AU). Both our CJS and EJS simulations have a median AMD smaller than the Chambers (2001) simulations, and for our EJS simulations, the value is 5 times smaller. Hence, our simulations continue the trend of decreasing the dynamical excitation of the terrestrial planets with increasing numbers of gravitationally interacting bodies, i.e., with increasing dynamical friction. Other potentially important variables, such as the assumed surface density profile, the 1:1 ratio between the mass placed in the embryo and planetesimal populations, and the presence of Jupiter and Saturn at the beginning of the simulation, are the same in our simulations as in Chambers (2001) Simulations 21–24.

3.4. Composition of final planets

The final planets are, on average, dominated by material supplied by embryos. For the CJS simulations, the 'median-composition' planet has 60% of its mass supplied by embryos, 20% supplied by planetesimals that have been accreted by those embryos, and 20% supplied by planetesimals that are directly accreted onto the planet.[1] For the EJS set of simulations, these values are similar: 62, 24, and 14%. There is, of course, some variation in these values from planet to planet, given the stochastic nature of the accretion process.

The individual planets tend to accrete most of their material from the region closest to them, but there is still a significant amount of radial mixing that occurs. We characterize the degree of radial mixing in each planetary system with the value σ, defined as

$$\sigma = \frac{\sum_i m_i |a_{\mathrm{fin},i} - a_{\mathrm{init},i}| / a_{\mathrm{fin},i}}{\sum_i m_i} \quad (3)$$

(Chambers, 2001) where m_i and $a_{\mathrm{init},i}$ are the masses and initial semi-major axes of each body that is accreted by a planet and $a_{\mathrm{fin},i}$ are the final semi-major axes of each body (i.e., the semi-major axis of the planet that the body is accreted by). Table 4 gives σ for the terrestrial planet systems formed in each of our simulations for all bodies as well as for just the planetesimal and embryo contributions. In calculating these values, bodies are counted individually even if they are first accreted by another embryo before ending up in the final planet. On average, there is more radial mixing in the CJS set of simulations than in the EJS set, and in both cases, planetesimals are gathered from a somewhat wider region than embryos, which is expected given the fact that they are more dynamically excited than the embryos due to dynamical friction.

Fig. 3 shows the makeup and relative sizes of the planets in all of our simulations. In the CJS set of simulations, the radial mixing is obvious, with many planets consisting of a substantial amount of material originating from beyond 2.5 AU (which we refer to here as the 'outer asteroid belt'). By comparison, in the EJS set of simulations there is a profound lack of material from beyond 2.5 AU in all but 1 of the planets, and even a relatively small contribution of material from the 2.0–2.5 AU zone for the majority of the planets. As we discuss further in Section 5, this difference is important in that material originating from beyond ∼2.5 AU is a potential source of the Earth's water and other volatiles (e.g., Morbidelli et al., 2000; Raymond et al., 2004).

Table 4
Degree of radial mixing in each of the simulations

	CJS			EJS		
	σ_{all}	σ_{sb}	σ_{emb}	σ_{all}	σ_{sb}	σ_{emb}
1	0.72	0.63	0.78	0.58	0.60	0.58
2	0.50	0.60	0.44	0.42	0.45	0.39
3	0.58	0.60	0.58	0.48	0.51	0.46
4	0.54	0.63	0.48	0.42	0.53	0.31
Median	0.56	0.61	0.53	0.45	0.52	0.43

The radial mixing statistic σ is calculated with Eq. (3) for all bodies that go into each planet (σ_{all}), as well as for the individual planetesimal (σ_{sb}, for 'small bodies') and embryo (σ_{emb}) contributions.

Fig. 4 shows the relative contributions of material from different regions inside 2.0 AU for the planets formed in the EJS set of simulations. From this figure, it is clear that even though there is little contribution of material from beyond 2.5 AU in the EJS simulations, radial mixing of material inside of 2 AU is still substantial. The CJS simulations experience a comparable amount of mixing of material within 2 AU.

Only 3 of the 12 planets in the CJS set of simulations do not contain any embryos from beyond 2.5 AU, 5 planets contain 1 such embryo, and 4 contain 2. In addition, each planet contains a median value of 7 directly-accreted planetesimals originating from beyond 2.5 AU and another 4 that were first accreted by a another embryo before ending up in the final planet. The relative mass fractions of material originating from beyond 2.5 AU that is delivered by embryos, directly-accreted planetesimals and pre-accreted planetesimals are 76, 16, and 8%, respectively (median for all CJS simulations). The fraction of each planet's total mass that originates from beyond 2.5 AU has a median value of 15% and ranges from 1.6 to 38%.

In contrast, with the exception of the one planet in simulation EJS3 that originated as an embryo beyond 2.5 AU and never accreted any other embryos, none of the final planets in the EJS simulations contain any embryos originating from beyond 2.5 AU. In addition, the median numbers of directly- and pre-accreted planetesimals originating from beyond 2.5 AU are both zero, with the sum never exceeding 3. The fraction of each planet's total mass that originates from beyond 2.5 AU (excluding the one single-embryo planet that originated from beyond 2.5 AU) has a median value of 0.3% and ranges from 0 to 1.6%, with 5 of the 14 planets containing no material at all from beyond 2.5 AU.

[1] When we refer to the fraction of a planet that is made of embryos and of planetesimals, we are referring to embryos and planetesimals that were present at the beginning of our simulations. Technically, the embryos that we start with at the beginning of our simulations would consist of planetesimals that have been accreted in the previous runaway and oligarchic growth phases, such that everything is ultimately made of planetesimals.

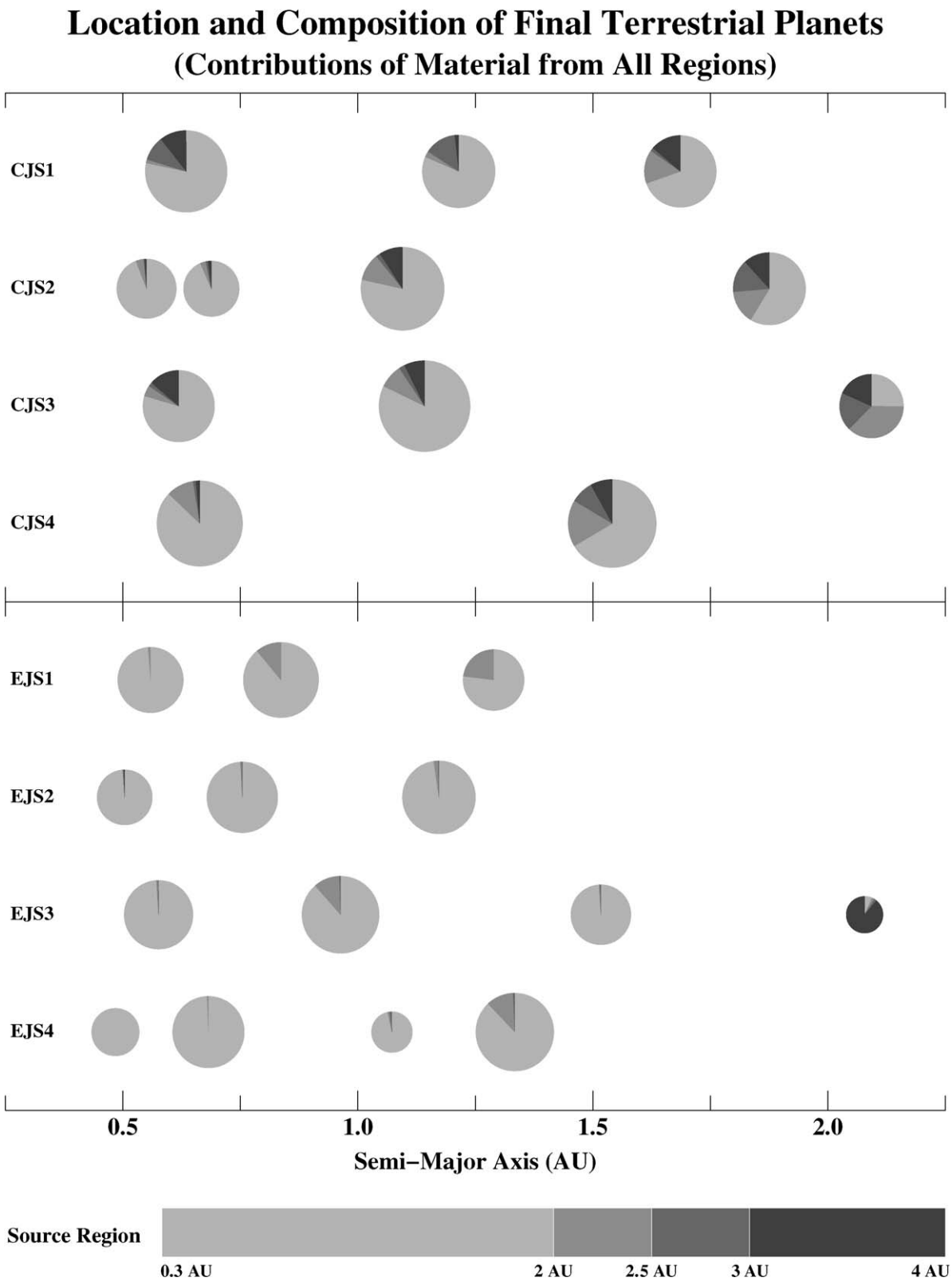

Fig. 3. Final terrestrial planets formed in all of our simulations. Pie diagrams show the contributions of material from the different semi-major-axis regions, and the diameter of each symbol is proportional to the diameter of the planet.

3.5. Timescales and characteristics of the accretion process

Table 5 gives the timescales for planets to grow to 50 and 90% of their final masses (t_{50} and t_{90}) in all of our simulations. It is interesting to note that the timescales for accretion are not strongly dependent on the final mass of the planet. There is, however, a clear dependence on the configuration of Jupiter and Saturn, with the accretion timescales being significantly

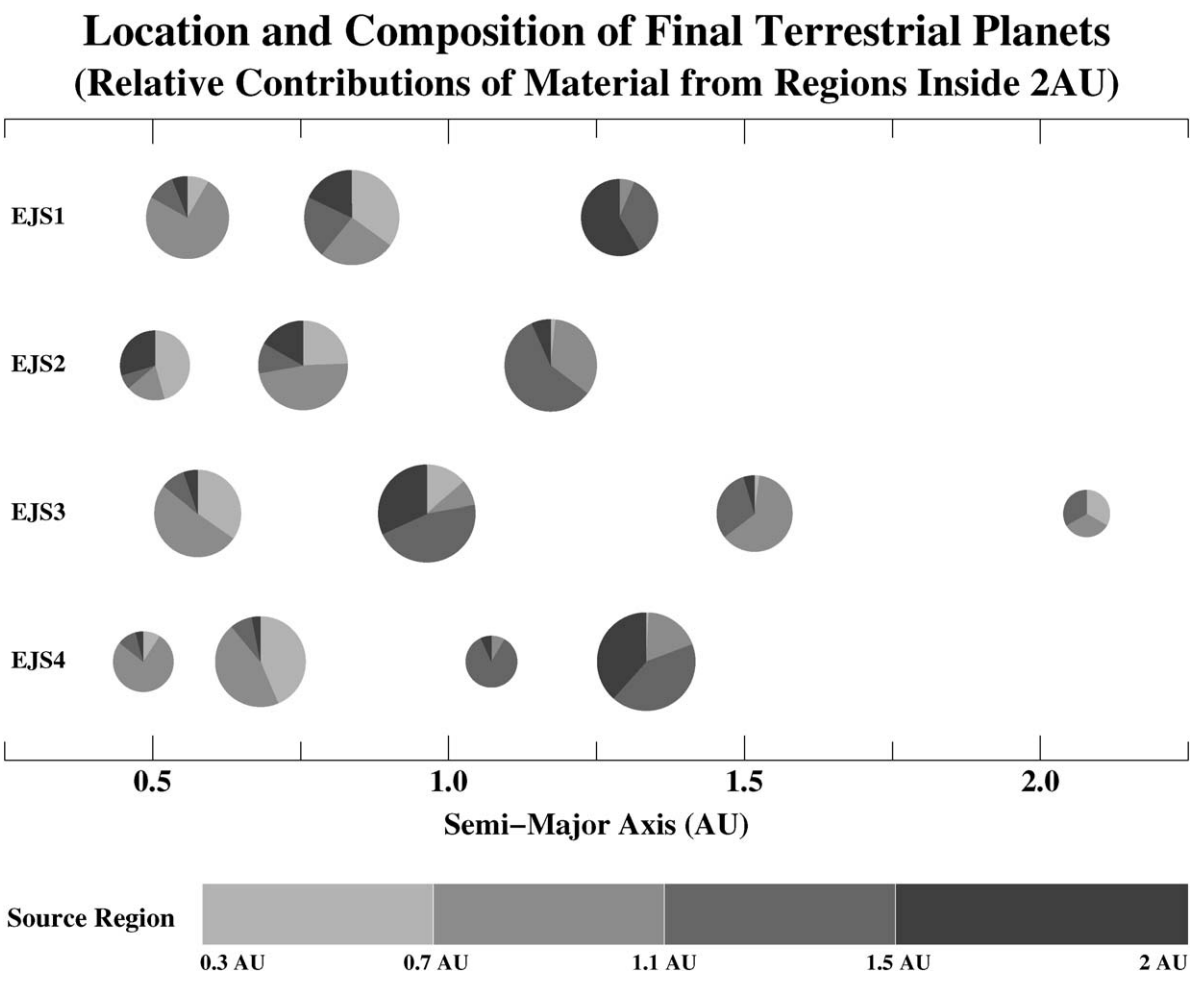

Fig. 4. Relative contributions of material from regions inside 2.0 AU for the planets formed in the EJS set of simulations. Pie diagrams show the relative contributions of material from the different semi-major-axis regions, and the diameter of each symbol is proportional to the diameter of the planet. While the planets in the CJS simulations are not shown here, they experience a comparable amount of radial mixing of material inside of 2.0 AU.

Table 5
Growth timescales for planets in all of our simulations

	M_{planet}	N	t_{50} (Myr), median (range)	t_{90} (Myr), median (range)
CJS	All	12	22 (6–109)	65 (25–196)
	$>0.50\,M_e$	10	23 (6–109)	69 (25–196)
	$>0.75\,M_e$	9	25 (8–109)	70 (25–196)
EJS	All	14	13 (0.005–25)	40 (0.15–182)
	All (>1 Embryo)	11	16 (4–25)	44 (24–182)
	$>0.50\,M_e$	8	16 (5–25)	40 (24–182)
	$>0.75\,M_e$	6	14 (5–25)	34 (24–76)

M_{planet} is the mass of the planet, N is the number of planets in the simulations that fall into a given mass range, and t_{50} and t_{90} are the timescales necessary for a planet to reach 50 and 90% of its final mass. The timescales do not depend strongly on the mass of the planets, but do depend on the configuration of Jupiter and Saturn.

longer in the CJS set of simulations than in the EJS simulations.

The statistics for final large impacts are shown in Table 6 for all planets consisting of two or more embryos at the end of the simulation. For the CJS simulations, all 12 of the final planets fall into this category, while for the EJS simulations, 3 of the 14 planets consist only of one embryo and some planetesimals, and are not counted in the table. A large impact is classified here as one in which the impactor is at least as large as a single embryo.

For the CJS set of simulations, the median value of t_{90} from Table 5 is smaller than the median time of the last large impact (t_{imp}) from Table 6, while for the EJS set of simulations, the median t_{90} is larger. This is due to the fact that larger planets are formed in the CJS simulations, such that the final embryo impact can sometimes deliver less than 10% of the final mass of the planet and hence occur after t_{90}. In the EJS simulations, no planets larger than an Earth mass are formed, and since the embryos have a mass of 0.0933 M_e (and generally accrete several planetesimals as well), there are no cases where the final embryo impact delivers less than 10% of the final mass of the planet.

We can compare our timescales to the results from previous simulations by other authors. Chambers and Wetherill (1998) found that in their Model C simulations extending to ∼4 AU and incorporating up to ∼50 bodies (starting with the current orbits of Jupiter and Saturn), the median time of the last impact is 125 Myr. Our EJS set of simulations yields a median t_{imp} that

Table 6
Statistics for final large impacts into each planet in all of our simulations

	$M_{\rm planet}$	N	$t_{\rm imp}$ (Myr), median (range)	$M_{\rm imp}$ (M_e), median (range)	V_∞ (km/s), median (range)	$M_{\rm veneer}$, median (range)
CJS	All	12	74 (13–232)	0.11 (0.1–0.21)	4.89 (1.0–27.5)	1.4% (0.0–16.4)
	>0.50 M_e	10	99 (25–232)	0.11 (0.1–0.21)	4.89 (1.0–27.5)	1.0% (0.0–8.9)
	>0.75 M_e	9	114 (25–232)	0.11 (0.1–0.21)	4.62 (1.0–27.5)	1.2% (0.0–8.9)
EJS	All (>1 Embryo)	11	34 (14–182)	0.13 (0.11–0.39)	4.65 (2.83–7.94)	7.1% (0.4–18.8)
	>0.50 M_e	8	31 (14–182)	0.15 (0.11–0.39)	4.06 (2.83–7.32)	10.2% (0.4–18.8)
	>0.75 M_e	6	26 (14–76)	0.13 (0.11–0.39)	4.06 (2.83–6.85)	10.2% (2.9–18.8)

A large impact is one in which the impactor is at least as large as a single embryo. $M_{\rm planet}$ is the mass of the planet, N is the number of planet in the simulations that fall into a given mass range, $t_{\rm imp}$ is the time of the final large impact, $M_{\rm imp}$ is the mass of the impactor, V_∞ is the velocity of the impactor at infinity (i.e., not taking gravitational focusing into account) and $M_{\rm veneer}$ is the mass of material accreted after the final large impact, relative to the total mass of the planet. Note that while the fastest large impact in the CJS simulations is at 27.5 km/s, it is somewhat of an anomaly—the next fastest impact is at 9.96 km/s.

is about a factor of 4 shorter than this. In the Chambers (2001) Simulations 21–24, which incorporate ∼150 bodies (and also assume the current orbits of Jupiter and Saturn), they found that the median times for the Earth and Venus analogues in their simulations to reach 90% of their final mass were 54 and 62 Myr, respectively. Their simulations extend only to 2 AU, and it is likely that if they were extended to 4 AU their timescales would be somewhat longer (e.g., Chambers and Wetherill (1998) find a median $t_{\rm imp}$ in their Model C simulations, which extend out to 4 AU, that is ∼50% larger than in their Model B simulations, which only extend to 1.8 AU). In comparison, we find a median t_{90} of ∼40 Myr in our EJS set of simulations. Our simulations thus continue the trend of decreasing accretion timescales with increasing numbers of bodies and hence increasing dynamical friction. Other potentially important variables, such as the assumed surface density profile, the 1:1 ratio between the mass placed in the embryo and planetesimal populations, and the presence of Jupiter and Saturn at the beginning of the simulation, are the same in our simulations as in Chambers (2001) Simulations 21–24.

Recent measurements using the ^{182}Hf–^{182}W isotope system (Halliday et al., 2000; Kleine et al., 2002; Yin et al., 2002) suggest that the Earth accreted and differentiated on a timescale of ∼10–30 Myr. There are some issues involved in the interpretation of Hf–W data for the Earth, such as the possibility that large impacts only lead to the partial resetting of the Hf–W system, so it has been suggested that the Hf–W dates for the Earth may be low by a factor of ∼2 (e.g., Halliday, 2004; Sasaki and Abe, 2004). However, Hf–W ages for the Moon's formation (likely due to the final large impact into the Earth), are less likely to be affected by issues such as partial resetting and seem to be converging to a value of ∼30 Myr (Halliday et al., 2000; Jacobsen and Yin, 2003).

Our EJS simulations yield timescales t_{90} and $t_{\rm imp}$ reasonably close to these Hf–W ages, while the timescales we find in our CJS set of simulations are a factor of a few larger. It is possible that some discrepancy is due to the interpretation of Hf–W data, as noted above. However, given the trends towards decreasing accretion timescales with increasing dynamical friction, the discrepancy between numerical models and the geochemical evidence will likely diminish in future simulations that incorporate even larger numbers of gravitationally interacting bodies and that include the regeneration of small bodies during large impact events (e.g., Agnor and Asphaug, 2004; Levison et al., 2005).

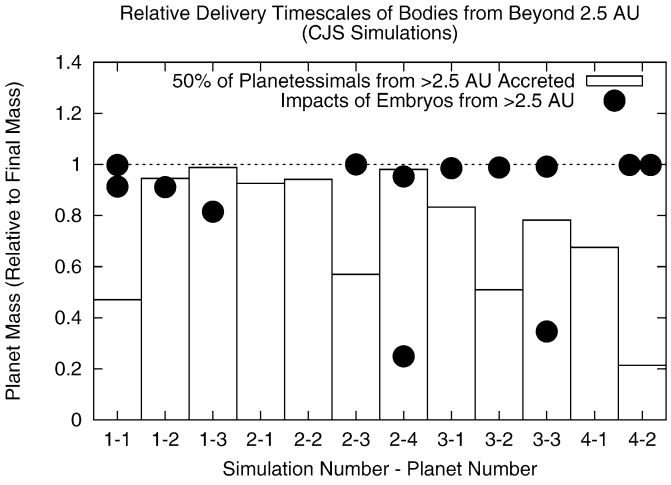

Fig. 5. Relative timing of the accretion of bodies originating from beyond 2.5 AU, which are likely to be carriers of water and other volatile material, in our CJS simulations. The bars show the mass of each planet, as a fraction of its final mass, at which 50% of the final number of planetesimals originating from beyond 2.5 AU have been accreted. The dots give the planet mass following the impact of embryos from beyond 2.5 AU. The impact on planet 4–2 is from a body consisting of 2 embryos from beyond 2.5 AU. Only 3 planets do not experience the impact of an embryo from beyond 2.5 AU. Planetesimals from beyond 2.5 AU that are accreted by another embryo before hitting the planet are not counted in this graph.

There is a significant difference between our two sets of simulations in terms of the relative amount of mass accreted after the last large impact, often termed the *late veneer*. From Table 6, $M_{\rm veneer}$, the fraction of a planet's mass that arrives after the last large impact, is nearly an order of magnitude larger in the EJS simulations than in the CJS simulations, roughly 10% compared to 1%. In the CJS simulations, the median mass fraction of material in the late veneer from beyond 2.5 AU, as a fraction of planet mass, is 0.7%, and ranges from 0–2.9% with 4 planets having 0%. For the EJS simulations, essentially no late veneer material originates from beyond 2.5 AU.

The final issue that we address with regards to accretion timescales in this section is the relative timing of the delivery of potentially volatile-rich material from beyond 2.5 AU. Fig. 5

shows, for each planet in the CJS set of simulations, the mass of the planet (relative to its final mass) at which 50% of its final number of planetesimals originating from beyond 2.5 AU have been accreted, as well as the planet mass following the accretion of any embryos from beyond 2.5 AU. Planetesimals from beyond 2.5 AU that are first accreted by another embryo before hitting the planet are not counted in this graph.

From Fig. 5, in the majority of cases, the 50% point of delivery of planetesimals from beyond 2.5 AU does not occur until well after the planet has grown to half its size. Similarly, nearly all of the embryo impacts occur well after the planet has grown to half of its mass. In fact, of the 9 planets that do experience at least one impact from an embryo from beyond 2.5 AU, 8 of those planets have such an embryo as their final large impactor. Thus, delivery of potential volatile-carrying material generally occurs late in a planet's growth, and in the case of volatile-carrying embryos, often as the final large impact. From Section 3.4, the relative mass fractions of material originating from beyond 2.5 AU that is delivered by embryos, directly-accreted planetesimals and pre-accreted planetesimals are 76, 16, and 8%, respectively (median for all CJS simulations).

As we discuss in Section 3.4, none of the planets in the EJS set of simulations experiences an impact from an embryo from beyond 2.5 AU. With the exception of the one planet that is essentially just an embryo that originated from beyond 2.5 AU, all of the other planets contain approximately 1% or less of material that originated from beyond 2.5 AU, and 5 out of the 14 planets have 0%. Hence, similar statistics to those presented in Fig. 5 cannot be made for the EJS simulations.

Fig. 6 shows the distributions of impact velocities for all of the bodies that impact planets in both sets of simulations. Impact velocities are plotted as a function of the time of the impact, and are the velocities at infinity (V_∞), which do not take gravitational focusing into account. From the figure, the impact velocity of planetesimals is roughly 3 times that of em-

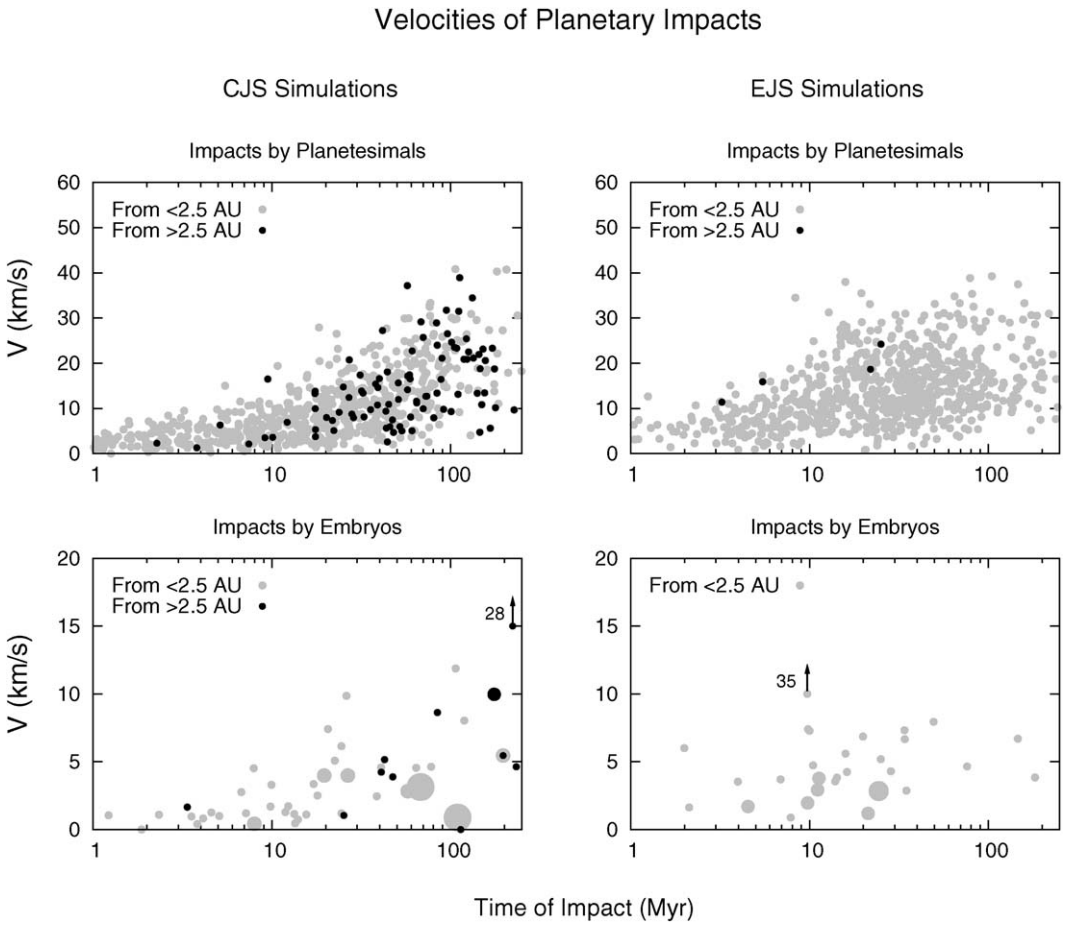

Fig. 6. Plot of the velocities of all planetary impactors in our simulations. Velocities are plotted versus the time of impact and are the values at infinity (V_∞), which do not take into account gravitational focusing. The arrows and numbers indicate two embryo impacts that are faster than the plotted range. The diameter of the symbols for the embryos is proportional to the mass of the embryo. Grey symbols are for material originating inside 2.5 AU and black symbols are for material from outside 2.5 AU. The gray symbol with a black dot in the center in the CJS embryo plot is a body consisting of one embryo from inside 2.5 AU and one from outside. Planetesimals impact the planets at roughly 3 times the speed of embryos in both sets of simulations. The velocity distributions of planetesimal impacts in the CJS and EJS sets of simulations are roughly similar, but there are few planetesimals originating from beyond 2.5 AU that hit any of the planets in the EJS set of simulations. The velocity distributions of embryo impacts in the two sets of simulations are noticeably different, with the average velocity remaining reasonably constant with time in the EJS simulations but growing with time in the CJS simulations. The early embryo impacts are at lower velocities in the CJS than in the EJS set of simulations, while the late impacts by embryos are faster in the CJS simulations, due in a large part to embryos from beyond 2.5 AU. There are no impacts from embryos originating beyond 2.5 AU in the EJS simulations.

bryos in both sets of simulations. The velocity distributions of planetesimal impacts in the CJS and EJS sets of simulations are roughly similar, although there are many impactors originating from beyond 2.5 AU in the CJS simulations and few in the EJS simulations. The velocity distributions of embryos, however, are noticeably different. Early impacts are at lower velocities in the CJS than in the EJS set of simulations, while the later impacts are at higher velocities in the CJS simulations, and no embryos originating from beyond 2.5 AU hit any of the planets in the EJS set of simulations.

4. Interpretation of results

The results presented in the previous section highlight a number of differences between our two sets of simulations, and between our simulations in general and previous numerical simulations. Here, we provide an interpretation of those differences. As noted throughout Section 3, essentially all improvements over previous simulations are due to the use of a much larger number of bodies in our simulations, and hence a much more realistic treatment of the effects of dynamical friction. In Section 4.1, we summarize the major differences between our simulations and previous simulations, and describe in greater detail how the effects of increased numbers of small bodies and dynamical friction lead to these improvements. In Section 4.2, we focus on the differences between our CJS and EJS sets of simulations, and describe in detail how and why these differences are the result of the different orbits of Jupiter and Saturn in the two sets of simulations.

4.1. Effects of higher resolution and stronger dynamical friction

Previous numerical simulations of terrestrial planet accretion (e.g., Chambers and Wetherill, 1998; Agnor et al., 1999; Chambers, 2001; Raymond et al., 2004) treated systems that began with no more than ∼200 bodies. Given recent advances in computing power, we are able to treat systems with ∼1000 interacting bodies, which, while still an approximation to the actual process of terrestrial planet accretion, is a significant improvement over previous work. The most significant effect of using a larger number of interacting bodies is that our simulations more accurately account for the effects of dynamical friction, in which the equipartition of energy between large and small bodies damps the relative velocities of the larger ones (e.g., Wetherill and Stewart, 1993).

As noted in the introduction, we have likely not reached the limiting case where the effects of dynamical friction are independent of the individual planetesimal mass. The simulations we perform here are still in the regime where decreasing the individual planetesimal mass while proportionately increasing their number (hence keeping the same surface mass density of planetesimals) causes the effects of dynamical friction to become more pronounced, and hence result in significant differences as compared to previous simulations such as Chambers (2001).

In Section 3.3, we find that, in terms of the relative angular momentum deficit, our planets are much less dynamically excited than those formed in previous direct N-body simulations, and in the case of the EJS simulations, are actually lower on average than the terrestrial planets in our Solar System. Our level of dynamical excitation is comparable to that found by Levison et al. (2005), who used an N-body integrator modified to follow swarms of small bodies using tracer particles.

The effect of dynamical friction on the dynamical excitation of the final planets can be easily understood. While they are accreting, the planets experience frequent gravitational interactions with the numerous smaller planetesimals. These planetesimals are dynamically excited by the planets, and in turn they damp the eccentricities and inclinations of the planets. The larger number of planetesimals in our simulations, compared to previous simulations, leads to more damping and hence final planets that are less dynamically excited than those formed in simulations with smaller numbers of bodies (e.g., Chambers and Wetherill, 1998; Chambers, 2001). The differences between the dynamical excitation of the planetary systems in our CJS and EJS simulations will be discussed in Section 4.2.

In Section 3.5, we find that our accretion timescales, both in terms of the time necessary for planets to grow to 90% of their mass and the time of the final large impact, are significantly shorter than in previous simulations. With more dynamical friction resulting from a larger population of gravitationally interacting bodies, the embryos and growing planets in our simulations have their orbits more strongly damped than in previous simulations. This lowers their relative velocities, increasing gravitational focusing and making them more efficient at accreting one another.

As we discuss in the introduction to Section 3, an embryo remains in the asteroid belt region in only one out of our 8 simulations. Previous simulations (e.g., Chambers and Wetherill, 1998, 2001) had embryos remaining in the asteroid belt in ∼1/3 of their simulations. Another significant difference from previous simulations is that in our EJS set of simulations, very little material from beyond 2.5 AU ends up in the final terrestrial planets, while previous simulations with an eccentric Jupiter and Saturn but substantially fewer bodies (e.g., Morbidelli et al., 2000; Raymond et al., 2004) found a much larger contribution of bodies from beyond 2.5 AU.

It is unlikely that these differences between our simulations and previous works are due to factors other than simply using a larger number of bodies. In particular, the formation time of Jupiter does not have a substantial effect. Chambers and Wetherill (1998) introduce Jupiter after 10 Myr, but Chambers and Wetherill (2001) start with it right at the beginning (as in our simulations), and both of these works end up with an embryo in the asteroid belt in ∼1/3 of their simulations. Similarly, in Morbidelli et al. (2000), Jupiter is inserted at 10 Myr, while in Raymond et al. (2004), all but 4 of their simulations start with Jupiter right at the beginning. Both of these works find a substantial contribution of material from beyond 2.5 AU to the final terrestrial planets when Jupiter and Saturn are on their present orbits.

Hence, we believe that the differences between our simulations and previous works with regards to embryos remaining in the asteroid belt and the delivery of material from beyond 2.5 AU to the terrestrial planets are fundamentally the result of the larger number of bodies in our simulations. In previous simulations that included either just massive embryos or embryos plus a smaller population of planetesimals than in our simulations, gravitational interactions between those bodies lead to a random walk in semi-major axis with larger and less frequent 'jumps' than in our simulations. We suspect that in those simulations, embryos in the asteroid belt region were more likely to jump over resonances, such as the 3:1 and 5:2 mean-motion resonances (MMR) with Jupiter and the ν_6 secular resonance with Saturn, than to be pushed into one. By avoiding resonances, those bodies were therefore more likely to remain on stable orbits in the asteroid belt or to gradually increase their orbital e until they enter the terrestrial planet region.

In our simulations, however, the 'jumps' are smaller and more frequent due primarily to the larger number of smaller planetesimals. We suspect, therefore, that compared to previous simulations, it is more likely in our simulations that embryos are pushed into a resonance rather than jumping over it. Once in a resonance, the embryo can be quickly removed from the system either by ejection or by crashing into the Sun. Hence, compared to previous simulations that included fewer bodies, fewer embryos remain on stable orbits in the asteroid belt in our simulations. Similarly, in our EJS simulations, fewer embryos from beyond 2.5 AU (zero, actually) survive long enough to be accreted into the final terrestrial planets than in previous simulations. Given the different eccentricities of Jupiter and Saturn in our CJS and EJS simulations, there are significant differences in the strengths of the major resonances (Morbidelli and Henrard, 1991; Moons and Morbidelli, 1993). This results in substantial differences between our two sets of simulations in terms of the evolution of embryos from beyond 2.5 AU, which will be discussed in further detail in Section 4.2.

4.2. *Effects of Jupiter and Saturn's orbits*

In Section 3.4 we find that there is a profound lack of material from beyond 2.5 AU (referred to here as the 'outer asteroid belt') that ends up in the final terrestrial planets in the EJS simulations as compared to the CJS simulations. This is evident in Fig. 3, and is also reflected in the lower σ values in the EJS as compared to the CJS set of simulations (Table 4). Chambers and Cassen (2002) and Raymond et al. (2004) find a similar relationship between the outer-asteroid-belt contribution and Jupiter's eccentricity, although as noted in Section 4.1, the much larger number of small planetesimals in our simulations increases the efficiency of clearing the asteroid belt such that while they still find a significant contribution of outer-belt material when Jupiter has its current eccentricity, we do not. A related issue is that many more bodies hit the Sun in our EJS simulations than in our CJS simulations, as shown in Tables 1 and 2.

These effects are a direct result of the increased strength of resonances such as the 3:1 and 5:2 MMRs with Jupiter and the ν_6 secular resonance with Saturn when those planets are on eccentric orbits (Morbidelli and Henrard, 1991; Moons and Morbidelli, 1993). Fig. 7 shows the paths of several embryos originating beyond 2.5 AU in our simulations. The top two plots are representative of bodies in the EJS simulations, which begin with an eccentric Jupiter. In the first plot, the embryo migrates due to gravitational interactions for a few Myr until it enters the 5:2 resonance and is rapidly ejected from the

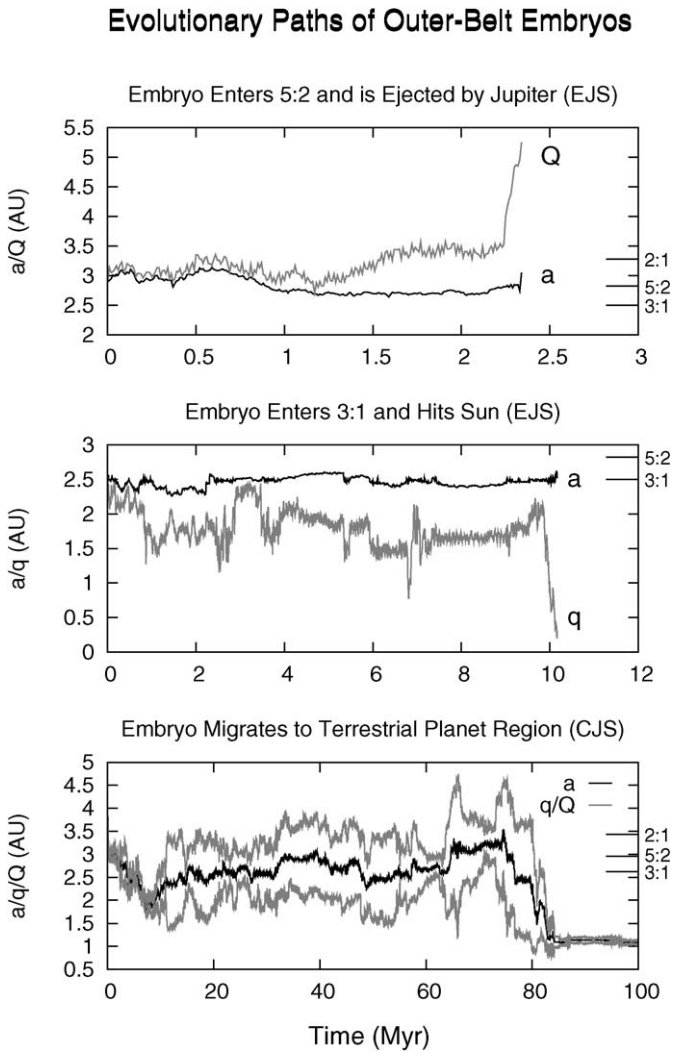

Fig. 7. Representative evolutionary paths for embryos originating beyond 2.5 AU in our simulations. The top two panels show embryos in the EJS set of simulations that enter resonances such as the 3:1 and 5:2 mean-motion resonance with Jupiter and are either ejected from the Solar System by Jupiter or crash into the Sun on short timescales. Such fates are common in the EJS set of simulations, and prevent essentially all embryos from beyond 2.5 AU from entering the terrestrial planet region. The bottom panel shows an embryo from the CJS simulations that, while occasionally passing through resonances and often briefly coming under their influence, migrates to the inner Solar System and accretes onto a terrestrial planet within 100 Myr. Such behavior is common in the CJS simulations, as resonances are substantially weaker given the nearly circular orbits of Jupiter and Saturn, and allows for a large number of embryos from the outer asteroid belt to accrete onto the final terrestrial planets. The result of this substantially different behavior is evident in the compositional differences between the final planets seen in Fig. 3. Note that the positions of the resonances in the CJS simulations are slightly different than those in the EJS simulations due to the different semi-major axes of Jupiter in the two sets of simulations.

system. In the second, the embryo enters the 3:1 resonance after about 10 Myr and quickly crashes into the Sun. The 3:1 and ν_6 resonances in particular are effective at increasing the eccentricity of bodies to the point where they hit the Sun (Farinella et al., 1994), which explains the much larger fraction of bodies in Tables 1 and 2 that hit the Sun.

In contrast, the lower plot of Fig. 7 shows a typical path of an embryo in the CJS simulations, which begin with Jupiter and Saturn on essentially circular orbits. The embryo migrates for about 100 Myr due to gravitational interactions, occasionally entering and leaving resonances, until it finally enters the terrestrial planet region and is accreted onto a planet at around 1 AU. Thus, the much weaker resonances in the CJS simulations allow for the survival of much more material from beyond 2.5 AU and hence allow for this material to end up in the final terrestrial planets. As we describe below, we believe that essentially all differences between our CJS and EJS simulations are the result of the fact that nearly all material from beyond 2.5 AU is removed from the system in the EJS simulations before it can accrete into the final terrestrial planets, whereas it contributes significantly in the CJS simulations.

In Section 3.3 we find that the planetary systems formed in the EJS set of simulations have, on average, a much lower dynamical excitation, as measured by the relative angular momentum deficit, than those in the CJS simulations. Very early in the simulations, the embryos are more excited in the EJS than in the CJS simulations, due to secular perturbations from the eccentric Jupiter and Saturn. This can be seen in Fig. 6, which shows that embryos impact the growing planets at higher velocities in the EJS than in the CJS simulations at times up to ∼6 Myr. However, Fig. 6 also shows that as time progresses the impact velocities of embryos hitting the planets in the CJS simulations begin to exceed those in the EJS simulations, in a large part due to the influx of material from beyond 2.5 AU. Excited embryos from beyond 2.5 AU, in addition to directly accreting onto the planets, will also excite other embryos that they gravitationally interact with, thus raising the overall level of dynamical excitation of the system.

The number of planetesimals that remain in the terrestrial planet region as a function of time is comparable in both sets of simulations, and decreases roughly exponentially with time. Hence, the damping of planetary eccentricities and inclinations by dynamical friction, at a given time, is comparable in both the CJS and EJS sets of simulations, and the level of damping will decrease with time. We believe that the larger dynamical excitation of the final terrestrial planets in the CJS simulations as compared to the EJS simulations is therefore due to the fact that the material making up the final terrestrial planets in the CJS simulations is on average more excited (due largely to the contribution of material from beyond 2.5 AU), and in addition that most excited material arrives at late times when there is less dynamical friction. Conversely, the lower dynamical excitation of the final planets in the EJS simulations is due to the fact that material from beyond 2.5 AU is ejected from the system early on, and hence very little of it is accreted into the final terrestrial planets.

In Section 3.2, we find that the CJS simulations produce systems with a smaller number of more massive planets that have a center of mass further from the Sun than in the EJS simulations (similar trends have been noted in previous simulations, e.g., Chambers and Cassen, 2002; Raymond et al., 2004). In Section 3.5 we find that the growth timescales for the planets, both in terms of the time necessary to grow to 90% of their mass (t_{90}) and the time of the final large impact ($t_{\rm imp}$), are larger in the CJS simulations than in the EJS simulations. Again, we believe that these differences are primarily the result of the rapid clearing of the region beyond ∼2.5 AU in the EJS simulations that we discuss above.

The fact that very little excited material from beyond 2.5 AU enters the terrestrial planet region in the EJS simulations leads to lower relative velocities amongst growing planets and planetary embryos, increasing their effective gravitational cross sections and accretion efficiency, and resulting in shorter growth timescales. The smaller total amount of mass available to build the planets in the EJS simulations, combined with the lower dynamical excitation of the embryos, means that the growing planets stake out a smaller range in semi-major axis over which they gather their material and hence allows a larger number of smaller planets to form than in the CJS simulations. Also, since the rapid clearing of material beyond 2.5 AU effectively reduces the center of mass of material available to form the terrestrial planets, it reduces the center of mass of the final planetary systems in the EJS simulations as compared to the CJS simulations.

We find that the average spacing of the planets in the two sets of simulations, in terms of their mutual Hill radii, is essentially the same. Hence, even though they are more numerous and are located closer to one another in absolute distance, the planets in the EJS simulations, due to their smaller average masses, are gravitationally separated from one another just as much as the more massive planets spread over a larger distance in the CJS simulations.

Finally, we find in Section 3.5 that the amount of material, termed the late veneer, that is accreted after the last large impact event is much larger in the EJS simulations than in the CJS simulations, and in both sets of simulations the late veneer consists predominantly of material originating from inside 2.5 AU. As noted above, planets form faster in the EJS than in the CJS simulations (in terms of $t_{\rm imp}$ and t_{90}), while the number of planetesimals that remain in the terrestrial planet region as a function of time is comparable in both sets of simulations. Hence, it follows that the planets in the EJS simulations will end up accreting more substantial late veneer of planetesimals than those in the CJS simulations.

5. Summary and implications

We have performed a suite of N-body integrations of the final stages of terrestrial planet formation that incorporate ∼1000 gravitationally interacting bodies, which is at least a factor of 5 more than in previous simulations. We performed 4 simulations, labeled EJS1-4, in which Jupiter and Saturn began on their present, eccentric orbits, and 4 simulations, labeled CJS1-4,

in which they began on the nearly circular and co-planar orbits predicted before the onset of the late heavy bombardment in the Nice Model (Gomes et al., 2005; Tsiganis et al., 2005; Morbidelli et al., 2005).

Because of the large number of bodies in our simulations, they account more accurately for the effects of dynamical friction than previous direct N-body integrations. Dynamical friction, in which the equipartition of energy between large and small bodies results in the damping of the relative velocities amongst the large bodies, is an important effect in planetary accretion (Wetherill and Stewart, 1993). It has already been shown to produce terrestrial planets with a dynamical excitation comparable to the terrestrial planets in our Solar System by Levison et al. (2005), using an N-body integrator modified to treat the effects of a swarm of small bodies using a set of tracer particles.

Our simulations have likely not reached the limiting case where the effects of dynamical friction are independent of the individual planetesimal mass. They are still in the regime where decreasing the individual planetesimal mass while increasing their number proportionately (hence keeping the same surface mass density of planetesimals) causes the effects of dynamical friction to become more pronounced, as can be seen in comparing our results to those from previous simulations, e.g., Chambers (2001).

Our direct N-body simulations produce final terrestrial planets that are less dynamically excited and accrete more quickly than in previous N-body simulations that included fewer bodies. Furthermore, the asteroid belt region in our EJS simulations is rapidly cleared of embryos, such that they are less likely to end up in the final terrestrial planets than in previous simulations with fewer bodies. We believe that the rapid clearing of material from the asteroid belt region in our EJS simulations as compared to our CJS simulations is the primary reason for the differences in the final planetary systems formed in those two sets of simulations. By comparing our simulations with a range of previous work, we have shown that our results seem to be due to the larger number of bodies in our simulations, and hence increased dynamical friction. Our results do not appear to be due to other factors, such as the presence of Jupiter and Saturn at the beginning of our simulations, which is also assumed in many previous works that we use for comparison (e.g., Chambers, 2001; Raymond et al., 2004).

While not an exact match, the final planetary systems formed in the EJS set of simulations are closer to those in our own Solar System in terms of number of planets, median planetary mass, and the center of mass of the system than those in the CJS simulations. They accrete faster than the planets in the CJS simulations, approaching the timescales estimated by Hf–W dating of the Earth's accretion and differentiation and the formation of the Moon. The dynamical excitation of the final planetary systems is also lower in the EJS simulations than in the CJS simulations, as explained in more detail in Section 4.2, with a median value even lower that of the terrestrial planets in our Solar System.

The trends that appear when comparing our simulations to previous simulations with smaller numbers of interacting bodies indicate that the timescales for accretion and the dynamical excitation of the final planetary systems will likely continue to decrease in future simulations that more accurately account for dynamical friction. It is also possible that the match between the numbers and masses of the planets formed in our CJS simulations and the terrestrial planets in our Solar System could be improved with stronger dynamical friction. By damping the growing planets and embryos even more than in our simulations, it is possible that the planets would accrete embryos from over a smaller range in semi-major axis and hence end up somewhat more numerous and less massive than those in our CJS simulations.

A more accurate treatment of dynamical friction could be achieved by incorporating even more gravitationally interacting bodies into our simulations, using tracer particles to approximate the effects of swarms of small bodies, and/or including the regeneration of small bodies during large impact events (e.g., Agnor and Asphaug, 2004; Levison et al., 2005). Regeneration of small bodies should be especially effective because the fragments generated from a large impact onto a growing planet would start on a similar orbit to the planet, and hence be dynamically cold relative to the planet. Thus, the initial conditions of our CJS simulations, and hence the Nice Model, cannot yet be ruled out on the issues of growth timescales, numbers and masses, and dynamical excitation of the terrestrial planets.

A potentially problematic issue, as described in Section 4.2, is that the better fit of the EJS simulations to the center of mass of our Solar System is due, at least in part, to the rapid clearing of the outer asteroid belt (beyond 2.5 AU). Given the weakness of the major resonances in the outer asteroid belt in our CJS simulations, it is uncertain whether the clearing efficiency of that region would be improved even if we added a large number of very small bodies to our simulations. Future simulations are necessary to solidly constrain how the center of mass of the final planetary systems changes with increasing resolution. It should also be noted that using a different initial surface density profile can potentially affect the final center of mass of the system. Likewise, other processes, such as secular resonance sweeping during the depletion of the solar nebula, can potentially lead to depletion of the asteroid belt region, especially the outer asteroid belt, and could potentially improve the fit of our CJS simulations in terms of the center of mass (Heppenheimer, 1980; Ward, 1981; Lemaitre and Dubru, 1991; Lecar and Franklin, 1997; Nagasawa et al., 2000).

Our simulations have important implications for the origin of the Earth's water. An influx of material from the outer Solar System late in the Earth's formation has been suggested as the primary source of its water and other volatiles (e.g., Chyba, 1987; Owen and Bar-Nun, 1995; Delsemme, 1997). However, the deuterium/hydrogen (D/H) ratio measured in comets of $309 \pm 20 \times 10^{-6}$ (Jessberger et al., 1988; Balsiger et al., 1995; Eberhardt et al., 1995; Meier et al., 1998; Bockelee-Morvan et al., 1998), or about $12\times$ the solar value of $25 \pm 5 \times 10^{-6}$ (Geiss and Gloeckler, 1998), is substantially larger than that of the D/H ratio of the Earth, which has a bulk D/H ratio of $149 \pm 3 \times 10^{-6}$, or about $6\times$ solar (Kyser and O'Neil, 1984; Bell and Rossman, 1992; Lécuyer, 1998). Because of this, and the inefficiency of accreting material on cometary orbits

(Levison et al., 2000), Morbidelli et al. (2000) concluded that cometary material can account for no more than ∼10% of the Earth's water budget.

However, the D/H ratio of carbonaceous chondrite meteorites is $159 \pm 10 \times 10^{-6}$ (with a range of 128–180 $\times 10^{-6}$), about 6× solar and consistent with the Earth's bulk value (Dauphas et al., 2000). The parent bodies of carbonaceous chondrites are estimated to have formed in the region beyond 2.5 AU, and carbonaceous chondrite meteorites can contain 1–10% by mass of water (Abe et al., 2000). By comparison, the water content of ordinary chondrites (formed around or inside 2.5 AU) is 0.3–3% and that of enstatite chondrites (formed around 2 AU) is $\lesssim$0.1% (Abe et al., 2000). The models of Morbidelli et al. (2000) and Raymond et al. (2004) found that the amount of material originating from the asteroid belt beyond 2.5 AU that ends up in the final terrestrial planets is capable of supplying the Earth's water budget and is consistent with measured D/H ratios on the Earth.

The mass of water in the Earth's crust, oceans, and atmosphere is 2.8×10^{-4} M_e, and the amount in the mantle is 0.8–8 $\times 10^{-4}$ M_e (Lécuyer, 1998). It has been suggested that 10–50 Earth oceans of water existed in primitive mantle (Dreibus and Waenke, 1989; Abe et al., 2000; Righter and Drake, 1999), although that amount has not yet been positively determined. Hence, a reasonable lower limit for the amount of water that must be delivered to the Earth is 5×10^{-4} M_e, while larger values would still be consistent given the uncertainty in the amount of water in the primitive mantle.

In our CJS simulations, the mass fraction of material from beyond 2.5 AU in the final terrestrial planets ranges from 1.6–38%, with a median value of 15%. Assuming that no volatiles are lost in the impact process and assuming a mass fraction of 10% water for the material originating from outside 2.5 AU, consistent with the values for carbonaceous chondrites, gives 0.0016–0.038 M_e of water for an Earth-sized planet, which is 3–75× the lower limit defined above (the median value is 0.015 M_e of water, or 30× the lower limit). Even assuming a more conservative mass fraction of water in the material beyond 2.5 AU of 5% and assuming that only 10% of the water is retained in the impact, the median amount of water in an Earth-mass planet is still 1.5× the lower limit. We find that, in the CJS simulations, the majority of a planet's water is delivered during embryo impacts that occur when it is close to its final mass, as also found by Morbidelli et al. (2000). Given that the planets' gravity will be stronger when they are close to their final sizes, this implies that a substantial fraction of the water is likely to be retained. We also find that relatively little water-bearing material is accreted after the last large impact occurs. The median mass fraction of material in the late veneer from beyond 2.5 AU, as a fraction of planet mass, is only 0.7% and ranges from 0–2.9%, with 4 of the 12 planets having 0%.

In contrast, the median mass fraction of asteroidal material from beyond 2.5 AU that ends up in the final terrestrial planets in our EJS simulations is 0.3%, with a maximum value of 1.6%. Essentially no late veneer material originates from beyond 2.5 AU. In the best-case scenario of perfect retention of all water in the impact and a 10% mass fraction of water in the impactors from beyond 2.5 AU, the majority of planets in the EJS simulations do not have the minimum amount of water necessary to be 'Earth-like.' The reasons for this are described in detail in Section 4.2, but it is fundamentally due to the fact that the stronger resonances with Jupiter and Saturn in the EJS simulations lead to a rapid clearing of embryos from the outer-asteroid-belt region, such that little of that material can make its way to the terrestrial planets. The clearing of embryos is aided by the large number of small planetesimals in our simulations, and thus while previous simulations incorporating fewer bodies (Morbidelli et al., 2000; Raymond et al., 2004) found that sufficient water could be delivered to Earth if Jupiter and Saturn are eccentric, we do not.

If Jupiter and Saturn did indeed start out on orbits as eccentric as they are today, an alternative source of water is likely necessary. Several mechanisms have been proposed, but remain to be fully quantified, e.g., the primordial capture of a hydrogen atmosphere around the Earth, some of which is oxidized into water (Sasaki and Nakazawa, 1990), delivery of water by interplanetary dust particles (Pavlov et al., 1999), inward migration of water-bearing phyllosilicates by gas drag (Ciesla and Lauretta, 2005), or the accretion of some type of hydrated material that forms inside of 2 AU (Drake and Righter, 2002).

The Earth's mantle is enriched in highly siderophile elements relative to what would be expected following core formation (e.g., Morgan et al., 2001), which is interpreted to be the result of a late veneer of material added to the Earth after core formation ceased. Drake and Righter (2002) suggest that this material must amount to less that ∼1% of Earth's total mass. The median mass fraction of late veneer material in our CJS simulations (here defined as material accreted after the last large impact by an embryo) is ∼1%, reasonably consistent with this estimate, while in the EJS simulations it is closer to 10%. Drake and Righter (2002) also note that the osmium isotope ratios in the Earth's mantle are similar to ordinary chondrites but different from carbonaceous chondrites (e.g., Meisel et al., 2001; Walker et al., 2002), suggesting an inner-asteroid-belt or terrestrial-planet-region source of the late veneer impactors. Four of the 12 planets in our CJS simulations have a late veneer with no material originating from beyond 2.5 AU, and are hence consistent with the late veneer material originating entirely in the inner-asteroid-belt or terrestrial-planet region.

Delivering a large amount of water through material from the outer asteroid belt (i.e., material similar to carbonaceous chondrites) in our CJS simulations does not pose a problem for the overall abundance of siderophile elements or the osmium isotope ratio of the Earth's mantle, concerns noted by Drake and Righter (2002). Such problems arise only if a large fraction of the Earth's water is delivered in the late veneer following core formation. In our CJS simulations, essentially all water is delivered to the planets before or during the last giant impact, such that highly siderophile elements accreted along with it will mostly be segregated into the core (under the reasonable assumption that the core continues to form up through the last giant impact). After that last large impact, as we note above, our CJS simulations produce a significant number of planets with a small late veneer of material originating entirely

inside of 2.5 AU (material like ordinary chondrites), such that the siderophiles that do end up in the mantle from that late veneer are consistent with both the total abundance of siderophiles and the isotopic ratios of osmium in the Earth's mantle today.

Giant impact events, such as those hypothesized to have formed the Moon (e.g., Cameron, 2000; Canup and Asphaug, 2001), occur frequently in our simulations, since by necessity the embryos we start with must either be ejected from the system or end up impacting the growing planets. Canup (2004) performed a wide range of hydrocode impact simulations and found that the most likely conditions for Moon-forming events involved an impactor with a mass of 0.11–0.14 M_e impacting with $V_\infty < 4$ km/s late in the Earth's formation, such the Earth was >95% of its final mass following the impact. From Table 6, both the CJS and EJS sets of simulations frequently have planets that are roughly Earth-sized (defined here as those larger than 0.75 M_e) and whose last large impact event is with a body ∼0.11–0.14 M_e at $V_\infty \lesssim 4$ km/s. The major difference between the two sets of simulations is that the Earth-sized planets in the EJS simulations have a median mass following the impact of about 90% of their final mass, while those in the CJS simulations are closer to 99% of their final mass, the latter being more consistent with the conditions found by Canup (2004). However, 1 out of the 6 Earth-sized planets in the EJS simulations does occur when the planet is >95% of its final mass, so the initial conditions of the EJS simulations cannot be ruled out conclusively on these grounds.

Wiechert et al. (2001) note that the oxygen isotope ratios in lunar samples fall along the same fractionation line as those of the Earth, which, using the numerical result of Canup and Asphaug (2001) that >80% of the material forming the protolunar disk comes from the impactor, is interpreted to indicate that the Moon-forming impactor must have been of the same composition as the Earth, and hence formed at roughly 1 AU. Similarly, Drake and Righter (2002) note that the differences in oxygen isotope ratios between the Earth–Moon system, Mars, and many meteorite types (except for enstatite chondrites, which are close to that of the Earth), indicate that the Earth and the protolunar impactor formed in the same region of the Solar System and the planets accreted material only from within a narrow range, and hence that there was little radial mixing during the accretion process.

However, we find that even with increased dynamical friction, the amount of radial mixing in our simulations is substantial (cf. Figs. 3 and 4). Even in the EJS simulations, where there is little contribution of material from the asteroid belt region to the final planets, there is substantial mixing of material within the terrestrial planet region. Even if the Moon-forming impactor did form around 1 AU, it would impact a proto-Earth consisting of material originating over a range of several AU. It is possible that stronger dynamical friction in our simulations might reduce the range over which embryos are accreted into the final planets, but at the same time it should expand the range over which planetesimals are accreted, and thus cannot by itself prevent substantial radial mixing. It appears that substantial radial mixing may be an unavoidable reality of the planetary accretion process.

A possible solution for reconciling simulations such as ours with the geochemical and cosmochemical data, at least for the Earth–Moon system, is that the material in the protolunar disk might equilibrate isotopically with the proto-Earth following the Moon-forming impact (D. Stevenson, pers. comm.). Alternatively, due to computational difficulties, hydrocode models of Moon-forming impacts only treat a non-rotating Earth, and thus they require a grazing impact to have a total angular momentum comparable to that of the Earth–Moon system. The grazing impact produces a protolunar disk that is primarily made of impactor material (e.g., Canup, 2004). In the case of a rapidly-rotating Earth, a moon-forming impact would be less grazing, so it is possible that the protolunar disk would form primarily of material from the Earth, and hence be much more similar in composition to the Earth. Both of these issues need to be explored in more detail.

We conclude by noting that our two sets of simulations are better than any previous simulations at matching the properties of the terrestrial planets in our Solar System. The still long accretion timescales and somewhat large dynamical excitation that we find in our CJS simulations will quite likely be lowered in future simulations with an improved treatment of dynamical friction. However, it is possible that even if we were to have stronger dynamical friction, having an eccentric Jupiter and Saturn might still be better for reproducing the number, masses, and center of mass of the terrestrial planets. At the same time, having Jupiter and Saturn on nearly zero-eccentricity orbits is better for providing water-bearing impactors from beyond 2.5 AU, providing a late veneer of material compatible with the siderophile element abundances and isotope ratios in the Earth's mantle, and having a potential Moon-forming impact occur when the Earth is nearly full-grown.

The Nice Model does not necessarily require a circular Jupiter and Saturn, but their initial eccentricities must be less than their current values or the system would immediately become unstable. As we note in Section 3.2, the initial eccentricities of Jupiter and Saturn in the EJS set of simulations decay to ∼0.01 over the first 50 Myr of the simulations due to gravitational interactions with material ejected from the system. It is thus possible that, in the Nice Model, Jupiter and Saturn could begin with eccentricities intermediate between 0 and their current values, although there is currently no well-defined model of how this could occur, and would decay to ∼0 well before the 2:1 resonance crossing 700 Myr later. In this case, the resulting system of terrestrial planets would be intermediate between those in our CJS and EJS simulations, and would potentially be a better overall fit to the full range of properties of the terrestrial planets in our Solar System.

Acknowledgments

We thank the anonymous reviewers for their helpful reviews and comments. D.P. O'Brien was supported by a Poincaré Fellowship at the Observatoire de la Côte d'Azur. This paper is PSI Contribution 397.

References

Abe, Y., Ohtani, E., Okuchi, T., Righter, K., Drake, M., 2000. Water in the early Earth. In: Canup, R.M., Righter, K. (Eds.), Origin of the Earth and Moon. Univ. of Arizona Press, Tucson, AZ, pp. 13–433.

Agnor, C., Asphaug, E., 2004. Accretion efficiency during planetary collisions. Astrophys. J. 613, L157–L160.

Agnor, C.B., Ward, W.R., 2002. Damping of terrestrial-planet eccentricities by density-wave interactions with a remnant gas disk. Astrophys. J. 567, 579–586.

Agnor, C.B., Canup, R.M., Levison, H.F., 1999. On the character and consequences of large impacts in the late stage of terrestrial planet formation. Icarus 142, 219–237.

Balsiger, H., Altwegg, K., Geiss, J., 1995. D/H and $^{18}O/^{16}O$ ratio in the hydronium ion and in neutral water from in situ ion measurements in Comet Halley. J. Geophys. Res. 100 (9), 5827–5834.

Bell, D.R., Rossman, G.R., 1992. Water in Earth's mantle: The role of nominally anhydrous minerals. Science 255, 1391–1397.

Bockelee-Morvan, D., Gautier, D., Lis, D.C., Young, K., Keene, J., Phillips, T., Owen, T., Crovisier, J., Goldsmith, P.F., Bergin, E.A., Despois, D., Wootten, A., 1998. Deuterated water in Comet C/1996 B2 (Hyakutake) and its implications for the origin of comets. Icarus 133, 147–162.

Cameron, A.G.W., 2000. Higher-resolution simulations of the giant impact. In: Canup, R.M., Righter, K. (Eds.), Origin of the Earth and Moon. Univ. of Arizona Press, Tucson, AZ, pp. 133–144.

Canup, R.M., 2004. Simulations of a late lunar-forming impact. Icarus 168, 433–456.

Canup, R.M.., Asphaug, E., 2001. Origin of the Moon in a giant impact near the end of the Earth's formation. Nature 412, 708–712.

Chambers, J.E., 1999. A hybrid symplectic integrator that permits close encounters between massive bodies. Mon. Not. R. Astron. Soc. 304, 793–799.

Chambers, J.E., 2001. Making more terrestrial planets. Icarus 152, 205–224.

Chambers, J.E., 2004. Planetary accretion in the inner Solar System. Earth Planet. Sci. Lett. 223, 241–252.

Chambers, J.E., Chambers, P., 2002. The effects of nebula surface density profile and giant-planet eccentricities on planetary accretion in the inner Solar System. Meteor. Planet. Sci. 37, 1523–1540.

Chambers, J.E., Wetherill, G.W., 1998. Making the terrestrial planets: N-body integrations of planetary embryos in three dimensions. Icarus 136, 304–327.

Chambers, J.E., Wetherill, G.W., 2001. Planets in the asteroid belt. Meteor. Planet. Sci. 36, 381–399.

Chyba, C.F., 1987. The cometary contribution to the oceans of primitive Earth. Nature 330, 632–635.

Ciesla, F., Lauretta, D., 2005. Radial migration and dehydration of phyllosilicates in the solar nebula. Earth Planet. Sci. Lett. 231, 1–2.

Dauphas, N., Robert, F., Marty, B., 2000. The late asteroidal and cometary bombardment of Earth as recorded in water deuterium to protium ratio. Icarus 148, 508–512.

Delsemme, A.H., 1997. The origin of the atmosphere and of the oceans. In: Thomas, P.J., Chyba, C.F., McKay, C.P. (Eds.), Comets and the Origin and Evolution of Life. Springer-Verlag, New York, pp. 29–67.

Drake, M.J., Righter, K., 2002. Determining the composition of the Earth. Nature 416, 39–44.

Dreibus, G., Waenke, H., 1989. Supply and loss of volatile constituents during the accretion of terrestrial planets. In: Atreya, S.K., Pollack, J.B., Matthews, M.S. (Eds.), Origin and Evolution of Planetary and Satellite Atmospheres. Univ. of Arizona Press, Tucson, AZ, pp. 268–288.

Duncan, M.J., Levison, H.F., Lee, M.H., 1998. A multiple time step symplectic algorithm for integrating close encounters. Astrophys. J. 116, 2067–2077.

Eberhardt, P., Reber, M., Krankowsky, D., Hodges, R.R., 1995. The D/H and $^{18}O/^{16}O$ ratios in water from Comet P/Halley. Astron. Astrophys. 302, 301–316.

Farinella, P., Froeschle, C., Froeschle, C., Gonczi, R., Hahn, G., Morbidelli, A., Valsecchi, G.B., 1994. Asteroids falling onto the Sun. Nature 371, 315–317.

Geiss, J., Gloeckler, G., 1998. Abundances of deuterium and helium-3 in the protosolar cloud. Space Sci. Rev. 84, 239–250.

Goldreich, P., Ward, W.R., 1973. The formation of planetesimals. Astrophys. J. 183, 1051–1062.

Gomes, R., Levison, H.F., Tsiganis, K., Morbidelli, A., 2005. Origin of the cataclysmic late heavy bombardment period of the terrestrial planets. Nature 435, 466–469.

Greenberg, R., Hartmann, W.K., Chapman, C.R., Wacker, J.F., 1978. Planetesimals to planets—Numerical simulation of collisional evolution. Icarus 35, 1–26.

Halliday, A.N., 2004. Mixing, volatile loss and compositional change during impact-driven accretion of the Earth. Nature 427, 505–509.

Halliday, A.N., Lee, D.-C., Jacobsen, S.B., 2000. Tungsten isotopes, the timing of metal-silicate fractionation, and the origin of the Earth and Moon. In: Canup, R.M., Righter, K. (Eds.), Origin of the Earth and Moon. Univ. of Arizona Press, Tucson, AZ, pp. 45–62.

Heppenheimer, T.A., 1980. Secular resonances and the origin of eccentricities of Mars and the asteroids. Icarus 41, 76–88.

Jacobsen, S.B., Yin, Q., 2003. Hf–W, accretion of the Earth, core formation and the origin of the Moon. Lunar Planet. Sci. XXXVV. Abstract 1913.

Jessberger, E.K., Christoforidis, A., Kissel, J., 1988. Aspects of the major element composition of Halley's dust. Nature 332, 691–695.

Kleine, T., Münker, C., Mezger, K., Palme, H., 2002. Rapid accretion and early core formation on asteroids and the terrestrial planets from Hf–W chronometry. Nature 418, 952–955.

Kokubo, E., Ida, S., 1996. On runaway growth of planetesimals. Icarus 123, 180–191.

Kokubo, E., Ida, S., 1998. Oligarchic growth of protoplanets. Icarus 131, 171–178.

Kominami, J., Ida, S., 2002. The effect of tidal interaction with a gas disk on formation of terrestrial planets. Icarus 157, 43–56.

Kominami, J., Ida, S., 2004. Formation of terrestrial planets in a dissipating gas disk with Jupiter and Saturn. Icarus 167, 231–243.

Kyser, T.K., O'Neil, J.R., 1984. Hydrogen isotope systematics of submarine basalts. Geochim. Cosmochim. Acta 48, 2123–2133.

Laskar, J., 1997. Large scale chaos and the spacing of the inner planets. Astron. Astrophys. 317, L75–L78.

Lecar, M., Franklin, F., 1997. The solar nebula, secular resonances, gas drag, and the asteroid belt. Icarus 129, 134–146.

Lécuyer, C., 1998. The hydrogen isotope composition of seawater and the global water cycle. Chem. Geol. 145, 249–261.

Lemaitre, A., Dubru, P., 1991. Secular resonances in the primitive solar nebula. Celest. Mech. Dynam. Astron. 52, 57–78.

Levison, H., Nesvorny, D., Agnor, C., Morbidelli, A., 2005. The role of dynamical friction in terrestrial planet formation. In: AAS/Division for Planetary Sciences Meeting Abstracts, vol. 37. Abstract 25.01.

Levison, H.F., Agnor, C., 2003. The role of giant planets in terrestrial planet formation. Astron. J. 125, 2692–2713.

Levison, H.F., Duncan, M.J., 2000. Symplectically integrating close encounters with the Sun. Astron. J. 120, 2117–2123.

Levison, H.F., Lissauer, J.J., Duncan, M.J., 1998. Modeling the diversity of outer planetary systems. Astron. J. 116, 1998–2014.

Levison, H.F., Duncan, M.J., Zahnle, K., Holman, M., Dones, L., 2000. Note: Planetary impact rates from ecliptic comets. Icarus 143, 415–420.

Meier, R., Owen, T.C., Jewitt, D.C., Matthews, H.E., Senay, M., Biver, N., Bockelee-Morvan, D., Crovisier, J., Gautier, D., 1998. Deuterium in Comet C/1995 O1 (Hale–Bopp): Detection of DCN. Science 279, 1707–1710.

Meisel, T., Walker, R.J., Irving, A.J., Lorand, J.-P., 2001. Osmium isotopic compositions of mantle xenoliths: A global perspective. Geochim. Cosmochim. Acta 65, 1311–1323.

Moons, M., Morbidelli, A., 1993. The main mean motion commensurabilities in the planar circular and elliptic problem. Celest. Mech. Dynam. Astron. 57, 99–108.

Morbidelli, A., Henrard, J., 1991. The main secular resonances nu6, nu5, and nu16 in the asteroid belt. Celest. Mech. Dynam. Astron. 51, 169–197.

Morbidelli, A., Chambers, J., Lunine, J.I., Petit, J.M., Robert, F., Valsecchi, G.B., Cyr, K.E., 2000. Source regions and time scales for the delivery of water to Earth. Meteor. Planet. Sci. 35, 1309–1320.

Morbidelli, A., Levison, H.F., Tsiganis, K., Gomes, R., 2005. Chaotic capture of Jupiter's Trojan asteroids in the early Solar System. Nature 435, 462–465.

Morgan, J.W., Walker, R.J., Brandon, A.D., Horan, M.F., 2001. Siderophile elements in Earth's upper mantle and lunar breccias: Data synthesis suggests manifestations of the same late influx. Meteor. Planet. Sci. 36, 1257–1276.

Nagasawa, M., Tanaka, H., Ida, S., 2000. Orbital evolution of asteroids during depletion of the solar nebula. Astron. J. 119, 1480–1497.

Owen, T., Bar-Nun, A., 1995. Comets, impacts and atmospheres. Icarus 116, 215–226.

Pavlov, A.A., Pavlov, A.K., Kasting, J.F., 1999. Irradiated interplanetary dust particles as a possible solution for the deuterium/hydrogen paradox of Earth's oceans. J. Geophys. Res. 104 (13), 30725–30728.

Petit, J., Morbidelli, A., Chambers, J., 2001. The primordial excitation and clearing of the asteroid belt. Icarus 153, 338–347.

Raymond, S.N., Quinn, T., Lunine, J.I., 2004. Making other earths: Dynamical simulations of terrestrial planet formation and water delivery. Icarus 168, 1–17.

Raymond, S.N., Quinn, T., Lunine, J.I., 2005a. High-resolution simulations of the final assembly of Earth-like planets. 1. Terrestrial accretion and dynamics. Icarus. In press.

Raymond, S.N., Quinn, T., Lunine, J.I., 2005b. High-resolution simulations of the final assembly of Earth-like planets. 2. Water delivery and planetary habitability. Astrobiology. Submitted for publication.

Righter, K., Drake, M.J., 1999. Effect of water on metal-silicate partitioning of siderophile elements: A high pressure and temperature terrestrial magma ocean and core formation. Earth Planet. Sci. Lett. 171, 383–399.

Sasaki, S., Nakazawa, K., 1990. Did a primary solar-type atmosphere exist around the proto-Earth? Icarus 85, 21–42.

Sasaki, T., Abe, Y., 2004. Partial resetting on Hf–W system by giant impacts. Lunar Planet. Sci. XXXV. Abstract 1505.

Thommes, E.W., Duncan, M.J., Levison, H.F., 2003. Oligarchic growth of giant planets. Icarus 161, 431–455.

Tsiganis, K., Gomes, R., Morbidelli, A., Levison, H.F., 2005. Origin of the orbital architecture of the giant planets of the Solar System. Nature 435, 459–461.

Walker, R.J., Horan, M.F., Morgan, J.W., Becker, H., Grossman, J.N., Rubin, A.E., 2002. Comparative ^{187}Re–^{187}Os systematics of chondrites—Implications regarding early Solar System processes. Geochim. Cosmochim. Acta 66, 4187–4201.

Ward, W.R., 1981. Solar nebula dispersal and the stability of the planetary system. I. Scanning secular resonance theory. Icarus 47, 234–264.

Ward, W.R., 2000. On planetesimal formation: The role of collective particle behavior. In: Canup, R.M., Righter, K. (Eds.), Origin of the Earth and Moon. Univ. of Arizona Press, Tucson, AZ, pp. 75–84.

Weidenschilling, S.J., 1980. Dust to planetesimals—Settling and coagulation in the solar nebula. Icarus 44, 172–189.

Weidenschilling, S.J., Cuzzi, J.N., 1993. Formation of planetesimals in the solar nebula. In: Levy, E.H., Lunine, J.I. (Eds.), Protostars and Planets III. Univ. of Arizona Press, Tucson, AZ, pp. 1031–1060.

Weidenschilling, S.J., Spaute, D., Davis, D.R., Marzari, F., Ohtsuki, K., 1997. Accretional evolution of a planetesimal swarm. Icarus 128, 429–455.

Wetherill, G.W., Stewart, G.R., 1989. Accumulation of a swarm of small planetesimals. Icarus 77, 330–357.

Wetherill, G.W., Stewart, G.R., 1993. Formation of planetary embryos—Effects of fragmentation, low relative velocity, and independent variation of eccentricity and inclination. Icarus 106, 190–209.

Wiechert, U., Halliday, A.N., Lee, D.-C., Snyder, G.A., Taylor, L.A., Rumble, D., 2001. Oxygen isotopes and the Moon-forming giant impact. Science 294, 345–348.

Wurm, G., Blum, J., Colwell, J.E., 2001. Note: A new mechanism relevant to the formation of planetesimals in the solar nebula. Icarus 151, 318–321.

Yin, Q., Jacobsen, S.B., Yamashita, K., Blichert-Toft, J., Télouk, P., Albarède, F., 2002. A short timescale for terrestrial planet formation from Hf–W chronometry of meteorites. Nature 418, 949–952.

Youdin, A.N., Shu, F.H., 2002. Planetesimal formation by gravitational instability. Astrophys. J. 580, 494–505.